The Canadian Mineralogist
Vol. 50, pp. 371-386 (2012)
DOI: 10.3749/canmin.50.2.371

ECLARITE: NEW DATA AND INTERPRETATIONS

DAN TOPA§

Department of Materials Research and Physics, Paris–Lodron University of Salzburg, Hellbrunnerstr. 34, A–5020 Salzburg, Austria

EMIL MAKOVICKY

Department of Geography and Geology, University of Copenhagen, Østervoldgade 10, DK–1350 Copenhagen, Denmark

ABSTRACT

The crystal structure of eclarite, first determined by Kupčík in 1984, has been refined on material from the scheelite deposit at Felbertal, Salzburg Province, Austria, to an R_1 value of 4.5% on the basis of 4141 unique reflections [$F_o > 4\sigma(F_o)$]. The chemical formula of material examined, based on 20.85 large cations (Z = 4) is $Cu_{0.76}Fe_{0.45}Ag_{0.12}Pb_{8.14}Bi_{12.59}S_{27.91}$; its unit-cell parameters are *a* 4.0307(1), *b* 22.7011(6), and *c* 54.615(1) Å, space group *Pmcn*. All the principal features of Kupčík's structure were confirmed. Three cation sites appear split into Pb and Bi subsites, and the octahedral site of the "cosalite-like" fragment is a partially occupied Bi site, flanked by three-fold coordinated, partly occupied Cu1 and Cu2 sites. The tetrahedral (Cu,Fe) site is split into a triangular position and a tetrahedral position. Replacement of Fe by Cu at the tetrahedral site and replacement of Bi by Cu at the octahedral site are positively correlated. They result in a general formula of eclarite equal to $Cu_{1.5n}Fe_{1-n}Pb_{9-1.25n}Bi_{12+n}S_{28}$ in which *n* is the molar proportion of the copper-based fully substituted ideal end-member $Cu_{1.5}Pb_{7.75}Bi_{13.0}S_{28}$, and (1–*n*), that of the Fe-based ideal end-member $FePb_9Bi_{12}S_{28}$. We propose a new interpretation of the crystal structure of eclarite, as a patchwork of large galenobismutite-like regions joined by interstitial elements.

Keywords: eclarite, sulfosalt, crystal structure, crystal chemistry, modular analysis.

INTRODUCTION

Eclarite, with an ideal structure formula (Cu,Fe)$Pb_9Bi_{12}S_{28}$, was described by Paar *et al*. (1983) as a new sulfosalt from Bärenbad, Achsel-Alm, Austria. It was found in quartz veins associated with chalcopyrite, pyrrhotite, sphalerite, stannite, joséite(?), bismuth, and gold. Kupčík (1984) determined its crystal structure, which he described as formed of galena-like units linked with one another partly as in cosalite and partly as in kobellite. He tried to illustrate these relations by setting together unit cells of eclarite, kobellite and cosalite with appropriate orientations and coordinates. The original structure was determined from 1838 observed reflections, with the resulting weighted R_1 value equal to 10.7° and isotropic displacement factors for all atoms.

Makovicky & Mumme (1985) gave a similar interpretation of the structure of eclarite using relations among rods, with simple substructures instead of unit cells. They defined continuous $(100)_{Ecl}$ slices of kobellite type, originally $\frac{1}{2}b_{Kob}$ thick, which alternatively, on every second contact, preserve the kobellite configuration, including the (Cu,Fe) site, whereas on alternative contacts, they are doubly truncated, rotated 180° and joined together, with the formation of a cosalite-like motif. The (Cu,Fe) tetrahedra are eliminated along these contacts. The cosalite-like amalgamation of rods involves the smaller type of rod present in the "parent" kobellite-like structure. Owing to the absence of Sb, these rods assume a PbS-like arrangement, distinct from that in true kobellite, in which they display an SnS-like internal configuration. The "half-kobellite" structure and composition of eclarite were stressed by Zakrzewski & Makovicky (1986) in the context of a calculation scheme for the electron-microprobe data of the minerals of the kobellite–izoklakeite homologous series.

Our main objective in this paper is to further refine the crystal structure of eclarite. Our findings furnish information on its finer aspects, contributing thus to the knowledge of the crystal chemistry of eclarite. Besides, interesting relations between the structures of eclarite and galenobismutite, independent of those between kobellite and eclarite, have been noticed and are described in some detail.

§ *E-mail address*: dan.topa@sbg.ac.at

Background Information

Occurrences of eclarite are rare. Pršek *et al.* (2008) described eclarite from Hviezda, the Low Tatras, Slovakia, and Topa (2001) described it from Felbertal, Austria. Material from the former occurrence was described with a formula $Cu_{1.20}Fe_{0.23}Ag_{0.11}Pb_{8.00}Bi_{11.15}Sb_{1.73}S_{28.59}$, whereas that from the Felbertal mine, and specifically orebody K3, has an empirical formula $Cu_{0.60}Fe_{0.57}Pb_{8.35}Ag_{0.17}Bi_{12.32}S_{27.93}$. The Ferbertal material used in this investigation is intergrown with cosalite and galenobismutite (Fig. 1).

Experimental

Chemical analyses

Quantitative chemical data for eclarite from its type locality at Bärenbad and from the Felbertal deposit were obtained with an electron microprobe, a JEOL Superprobe JXA–8600 installed at the Department of Geography and Geology, University of Salzburg. The apparatus was operated at 25 kV and 35 nA; measurement time was 15 s for peak and 5 s for background counts. The following standards and X-ray lines were used: natural $CuFeS_2$ (chalcopyrite; Cu*K*α, Fe*K*α), natural PbS (galena Pb*L*α), synthetic Bi_2S_3 (Bi*L*α, S*K*α), stibnite (Sb*L*α), synthetic CdTe (Cd*L*α, Te*L*α) and Ag metal (Ag*L*α). The raw data were corrected with the on-line ZAF–4 procedure.

Electron-microprobe analyses of eclarite reveal its fairly constant chemical composition, yielding an average result of 12 point analyses of the material used for single-crystal study as follows: Cu 0.92(5), Ag 0.25(3), Fe 0.47(3), Pb 31.56(31), Cd 0.20(3), Bi 49.44(24), Sb 0.22(3), Te 0.32(6), and S 16.86(7), for a total of 100.24(18) wt% (Table 1). This results in the following chemical formula of the mineral, based on 20.85 large cations ($Z = 4$) indicated by our refinement of the structure: $Cu_{0.76}Fe_{0.45}Ag_{0.12}Pb_{8.14}Bi_{12.59}S_{27.91}$. If Cu and Fe are lumped together as in the kobellite–izoklakeite series (Miehe 1971, Zakrzewski & Makovicky 1986, Moëlo *et al.* 1995) and if Ag with an equivalent amount of Bi is converted into Pb, the idealized formula reads $(Cu,Fe)_{1.21}Pb_{8.38}Bi_{12.47}S_{28}$. A surplus of (Cu,Fe) with respect to the ideal formula with these cations in a tetrahedral coordination is noted (Figs. 2, 3); further treatment of this problem is referred to in the section following the structure refinement.

Single-crystal X-ray diffraction

For our single-crystal investigation, several grains of eclarite were extracted from the galenobismutite–eclarite mixture (as shown in Fig. 1a). They were investigated with a Bruker AXS P3 diffractometer equipped with a CCD area detector using graphite-monochromated Mo*K*α radiation. An irregular fragment measuring approximately $0.05 \times 0.05 \times 0.15$ mm was found to be suitable for a structural investigation. Experimental data are listed in Table 2. The SMART (Bruker AXS 1998a) system of programs was used for unit-cell determination and data collection, SAINT+ (Bruker AXS 1998b) for the calculation of integrated intensi-

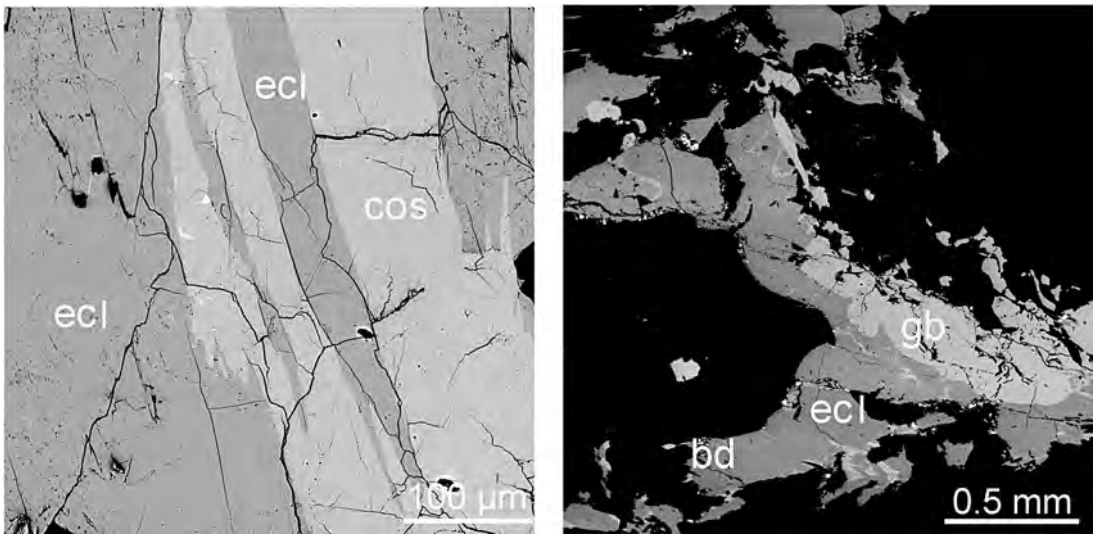

FIG. 1. The eclarite-containing association from the Felbertal tungsten deposit in back-scattered electron images. Symbols: ecl: eclarite, cos: cosalite, gb: galenobismutite, and an exsolution aggregate of bismuthinite derivatives (bd).

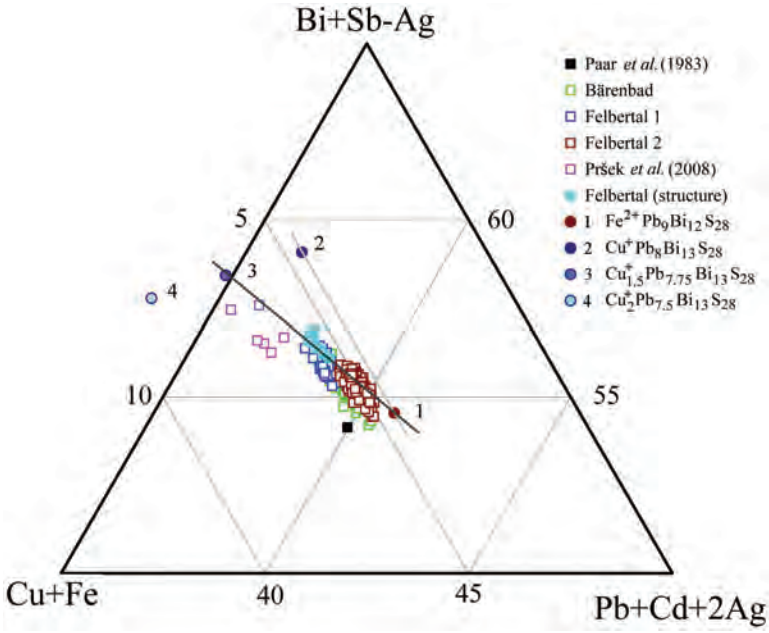

FIG. 2. Results of individual electron-microprobe analyses of eclarite performed in this study as well as the data published by Paar *et al*. (1983) and Pršek *et al*. (2008). The displacement and trend of the results, as well as the meaning of the four model compositions indicated, are discussed in the text.

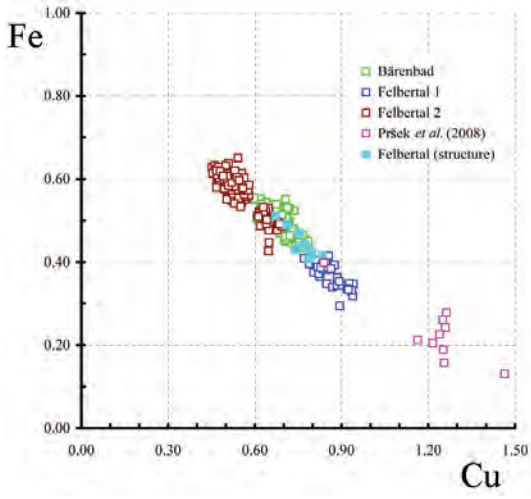

FIG. 3. Inverse correlation of the copper and iron contents per formula unit of eclarite derived from the current electron-microprobe data and from the data of Pršek *et al*. (2008). Details and interpretation are presented in the text.

ties, and XPREP (Bruker AXS 1998c) for empirical absorption correction based on pseudo Ψ-scans. The space group *Pmcn*, proposed by the XPREP program, was accepted. The structure of eclarite was solved by direct methods (program SHELXS: Sheldrick 1997a) and difference-Fourier syntheses (program SHELXL: Sheldrick 1997b). The labeling of the atoms (which had to be altered from the labeling scheme of Kupčík (1984) because of the new interpretations of several cation sites) is presented in Figure 4, and the structure is shown in Figure 5. Information about the refinement is given in Table 2; fractional coordinates of the atoms, and isotropic or anisotropic displacement parameters are listed in Table 3 (together with the parallel labeling scheme of Kupčík).

The quality of the structure refinement allows reliable interpretations, with R_1 equal to 0.045 for 4141 observed reflections, and a *wR* value of 0.101. Selected *Me*–S bond distances are presented in Table 4, and selected geometrical parameters for individual coordination-polyhedra, calculated with program IVTON (Balić-Žunić & Vicković 1996), are given in Table 5. A table of structure factors for eclarite may be obtained from the Depository of Unpublished Data on the MAC website [document Eclarite CM50_371].

The unit-cell dimensions of the present material are nearly identical to those given by Kupčík (1984)

TABLE 1. THE COMPOSITION OF ECLARITE FROM VARIOUS OCCURRENCES

No.	sample	NA	Cu	Ag	Fe	Pb	Cd	Bi	Sb	Te	S	total
1	Paar	1	0.90	0.20	0.60	34.20	0.00	45.60	1.50	0.00	17.20	100.20
2	Bärenbad	93	0.84	0.40	0.53	32.63	0.17	47.07	1.53	0.02	17.10	100.31
			0.05	0.09	0.03	0.46	0.11	0.70	0.39		0.23	0.39
3	Felbertal 1	35	1.05	0.45	0.40	31.64	0.21	49.54	0.38	0.00	16.78	100.44
			0.06	0.06	0.03	0.26	0.11	0.15	0.06		0.15	0.39
4	Felbertal 2	134	0.67	0.31	0.61	32.93	0.17	48.41	0.44	0.00	16.88	100.41
			0.08	0.05	0.05	0.26	0.11	0.44	0.28		0.22	0.39
5	structure	12	0.92	0.25	0.47	31.56	0.20	49.44	0.22	0.32	16.86	100.24
			0.05	0.03	0.03	0.31	0.03	0.24	0.03	0.06	0.07	0.18
6	Pršek	10	1.49	0.21	0.25	31.72	0.00	44.64	3.95	0.00	17.54	99.79
			0.17	0.10	0.08	0.56		1.35	0.81		0.36	0.31

No.	sample	*ch*	*ev*	Σ*Me*	Cu'	M'	C'/M'	Ref.
1	Paar	-1.42	-1.27	22.16	0.31	0.15	2.04	1
2	Bärenbad	0.08(1.7)	0.09(1.5)	22.04	0.19	0.15	1.26	2
3	Felbertal 1	1.91(0.95)	1.73(0.86)	22.08	0.23	0.15	1.53	2
4	Felbertal 2	0.96(2.1)	0.88(1.8)	21.97	0.12	0.15	0.79	2
5	structure	0.01(0.5)	0.01(0.5)	22.06	0.21	0.15	1.38	2
6	Pršek	-1.59(2.5)	-1.39(2.3)	22.30	0.45	0.15	3.00	3

1) $Cu_{0.74}Fe_{0.56}Ag_{0.10}Pb_{8.66}Bi_{12.09}S_{28.14}$ $(Cu,Fe)_{1.31}Pb_{8.85}Bi_{11.99}S_{28.14}$
2) $Cu_{0.69}Fe_{0.50}Ag_{0.19}Pb_{8.28}Bi_{12.38}S_{27.77}$ $(Cu,Fe)_{1.19}Pb_{8.67}Bi_{12.18}S_{27.77}$
3) $Cu_{0.86}Fe_{0.37}Ag_{0.22}Pb_{8.08}Bi_{12.55}S_{27.35}$ $(Cu,Fe)_{1.23}Pb_{8.52}Bi_{12.33}S_{27.35}$
4) $Cu_{0.55}Fe_{0.57}Ag_{0.15}Pb_{8.39}Bi_{12.31}S_{27.54}$ $(Cu,Fe)_{1.12}Pb_{8.76}Bi_{12.15}S_{27.54}$
5) $Cu_{0.76}Fe_{0.45}Ag_{0.12}Pb_{8.14}Bi_{12.59}S_{27.91}$ $(Cu,Fe)_{1.21}Pb_{8.38}Bi_{12.47}S_{27.91}$
6) $Cu_{1.22}Fe_{0.23}Ag_{0.10}Pb_{7.96}Bi_{12.79}S_{28.45}$ $(Cu,Fe)_{1.45}Pb_{8.16}Bi_{12.69}S_{28.45}$

The compositions are expressed in wt.% (standard deviation in second line). The empirical formulae were calculated on the basis of (Ag + Pb + Cd + Bi + Sb) = 20.85 *apfu*. NA: number of analyses. Standard deviation in terms of the last digit is shown in parentheses. The parameters *ch* and *ev* express the absolute and relative error in the charge balance based on the sum of cation and anion charges. Σ*Me* represents 20.85 *apfu* (heavy-metal site) plus Cu and Fe. Cu' is equal to Cu + Fe – 1, and M' is the missing 0.15 *Me* from the structure. References: 1) Paar *et al.* (1983), 2) this study, 3) Pršek *et al.* (2008).

(indicated here in square brackets): *a* 4.031 [4.030] Å, *b* 22.701 [22.75] Å, and *c* 54.615 [54.76] Å. The space group is *Pmcn* (no. 62); Kupčík (1984) used the conventional *Pnma* setting.

Description of the Structure

The crystal structure of eclarite has 24 independent cation positions, from which four are split into two subsites, and three have a partial occupancy. Bond distances indicate eight bismuth sites, five mixed (Bi,Pb) positions, and five lead sites among the non-split sites, and in addition, three potential Pb,Bi split sites, one tetrahedral site with a split Cu,Fe occupancy, and two partially occupied trigonal planar sites, Cu1 and Cu2. One large cation position, *Me*1, has partial occupancy as well. There are 28 fully occupied sulfur positions present. With regard to the *y* and *z* coordinates, all atoms are in a general position; *x* is equal to 0.25 and 0.75.

The structure can best be described by reference to two types of rod already defined in the structure of kobellite (Miehe 1971): (a) (parts of) dumbbell-shaped rods with an internal structure based on the PbS archetype, comprising 12 coordination polyhedra of large cations, and (b) smaller rods with a lozenge-like cross-section, comprising eight such polyhedra. All three positions involving copper are interstitial to these rods. The *Me*2 position between two dumbbell rods is interstitial as well.

The first type of rod is limited by pseudotetragonal surfaces that are three coordination pyramids wide (hosting Pb3, Pb2, and *Me*5, as well as Pb5, Pb7, and Pb8, respectively), and short pseudohexagonal surfaces formed respectively by S13, S14, S15 and S25, S26, and S27 (Fig. 4). With the exception of *Me*5, the above cations are trigonal prismatic sites. Irregularly shaped octahedral sites of bismuth Bi5–8 are situated in the thicker portions of the dumbbell rod, four-atomic-layers thick. In the thinner portions, which are three-atomic-planes thick, all cation sites are mixed (*Me*3, *Me*4, *Me*5, *Me*7a or *Me*7b, and *Me*8a or *Me*8b). The *Me*2 site, closing the dumbbell in a way not observed in kobellite

but present in cosalite (Srikrishnan & Nowacki 1974), appears to be an evenly mixed Pb,Bi site as well.

The inner cations of the rods with a lozenge-like cross-section, Bi1–Bi4, are typical asymmetric BiS1 + 2 + 2(+ 1) sites. Rods are only two pseudotetragonal coordination pyramids wide, and Pb1 and Pb4 on their surfaces are in a trigonal prismatic coordination. The mixed *Me*6a, *Me*6b site (the latter with bond characteristics intermediate between Pb and Bi) is situated close to the mixed sites 7 and 8 as well as to the mixed-occupancy Cu,Fe tetrahedron.

Two adjacent lozenge-shaped rods are connected in a cosalite-like manner (rod-layer type 3 of Makovicky 1993). The octahedrally coordinated cations playing a role in this interconnection ("*via* two octahedra that share edges") are *Me*1 with a slightly asymmetric octahedral coordination (three bonds of the order of 2.75 Å and three bonds of 2.88 Å, Table 4). The site *Me*1 is partially occupied (occupancy of 0.854, Table 3) and flanked by two sites occupied by small cations, a warped-trigonal site Cu1 and a planar-trigonal site Cu2. They have low occupancies (0.11–0.18). These are clearly bound to two different configurations of the interconnected lozenge motif, to its concave wall and to its straight wall, respectively. For every vacant octahedron of *Me*1, the sum of the occupancies of Cu1 and Cu2 shows that, within the accuracy of the refinement for such minor positions, the two opposing triangular walls can be occupied simultaneously. The Cu–S distances observed (Table 4) are influenced by the fact that in 85% of the cases, the octahedron size is determined by the large cation, and the S positions obtained are a weighted average of those required by *Me*1 and those required by Cu1 and Cu2. A potential partial replacement of Cu by Ag at the Cu1 site will lower somewhat the occupancy value obtained. The cosalite-like "bridge" just described is flanked on both sides by coordination octahedra of a mixed site *Me*5 (Fig. 4), in the same manner as in cosalite (Topa & Makovicky 2010).

The tetrahedral Cu,Fe site, with about equal contents of Cu and Fe, is split into a trigonal position, which can be assigned to Cu (2.29–2.33 Å) and a distorted tetrahedral position, which can be assigned to Fe (2.27–2.37 Å). It is analogous to such a site in kobellite (Miehe 1971) and izoklakeite (Makovicky & Mumme 1985, Armbruster & Hummel 1987) and to a similar site in kupčíkite (Topa *et al.* 2003).

TABLE 2. SINGLE-CRYSTAL X-RAY DIFFRACTION OF ECLARITE: EXPERIMENTAL AND REFINEMENT DETAILS

Crystal data	
Chemical formula	$(Cu,Fe)_{4.84}Ag_{0.48}Pb_{33.52}Bi_{49.88}S_{111.64}$
Formula weight	21442
Crystal system	Orthorhombic
Space group	*Pmcn* (#62)
Unit-cell parameters	
a, *b*, *c* (Å)	4.0307(1), 22.7011(6), 54.6145(13)
α, β, γ (°)	90, 90, 90
V (Å^3), *Z*	4997.3(2), 1
No. of reflections for cell param.	2216
D_x (g/cm^3)	7.125
μ (mm^{-1})	74.1
Crystal shape	irregular
Crystal color	metallic grey
Crystal size (mm)	0.05 × 0.05 × 0.15
Data collection	
T_{min}, T_{max}	0.0043, 0.0391
No. of measured reflections	34772
No. of independent reflections	4976
No. of observed reflections	4141
Criterion for observed reflections	$I > 2\sigma(I)$
R_{int}, R_σ (%)	10.7, 5.7
θ_{max}, θ_{max} (°)	0.75, 25.2
Range of *h*, *k*, *l*	$-4 \le h \le 4$, $-26 \le k \le 26$, $-64 \le l \le 64$
Refinement	
Refinement on F_o^2	
R [$F_o > 4\sigma(F_o)$] (%)	4.543
$wR(F_o^2)$ (%)	10.1
S (*GooF*)	1.032
No. of reflections used in refinement	4141
No. of parameters refined	323
Weighting scheme	a = 0.048, b = 0.0
	$w = 1/[\sigma^2(F_o^2) + (aP)^2 + bP]$, where $P = (F_o^2 + 2F_c^2)/3$
$(\Delta/\sigma)_{max}$	0.001
$\Delta\rho_{max}$ (e/Å^3)	2.70 (0.85 Å from Pb3)
$\Delta\rho_{min}$ (e/Å^3)	-2.26 (1.85 Å from Pb6B)
Extinction coefficient	0.000002(3)
Source of atomic scattering factors	*International Tables for X-Ray Crystallography* (1992, Vol. C, Tables 4.2.6.8 and 6.1.1.4)
Computer programs	
Structure solution	*SHELXS97* (Sheldrick 1997a)
Structure refinement	*SHELXL97* (Sheldrick 1997b)

Crystal Chemistry

The dual role of copper

Results of the present detailed determination of the crystal structure can now be confronted with results of the chemical analyses. We shall use a portion of the (Cu+Fe) – (Pb+Cd+2Ag) – (Bi+Sb–Ag) diagram (Fig. 2), in which silver was effectively eliminated from model calculations by a back-substitution Ag + Bi → 2Pb because of the scattered, fundamentally random character of its trace contents in the analyses (Table 1), and a Cu *versus* Fe diagram plotted in terms of atoms *pfu* (Fig. 3).

In the Cu *versus* Fe diagram, the inverse linear trend gives a least-squares fit: atoms Fe *pfu* = –0.583(11) atoms Cu *pfu* + 0.898(7), with standard errors for the two coefficients equal to 0.011 and 0.008, respectively, and the correlation coefficient R^2 equal to 0.902. This yields 0.90 atoms Fe *pfu* for an idealized Cu-free composition and 1.541 atoms Cu *pfu* for an ideal iron-free end-member. The latter corresponds to 0.54 atoms Cu *pfu* in the Cu1 + Cu2 sites, *i.e.*, 0.27 Bi *pfu* liberated from the octahedral *Me*1 (bismuth) position.

TABLE 3. COORDINATES, SITE OCCUPANCY, EQUIVALENT AND ANISOTROPIC DISPLACEMENT PARAMETERS (Å^2) OF ATOMS IN ECLARITE

Atom	K1984*	*x*	*y*	*z*	sof	$U_{eq/iso}$	U_{11}	U_{22}	U_{33}	U_{23}
Bi1	Bi1	0.75	0.14778(4)	0.07009(2)		0.0244(2)	0.0256(5)	0.0255(5)	0.0219(5)	-0.0008(4)
Bi2	Bi2	0.75	0.33131(4)	0.06587(2)		0.0245(2)	0.0258(5)	0.0259(5)	0.0218(5)	0.0006(4)
Bi3	Bi3	0.25	0.22287(4)	0.12551(2)		0.0247(2)	0.0248(5)	0.0285(5)	0.0209(5)	-0.0011(4)
Bi4	Bi4	0.25	0.40900(4)	0.12321(2)		0.0251(2)	0.0241(5)	0.0290(5)	0.0221(5)	-0.0010(4)
Bi5	Bi5	0.25	0.03474(4)	0.24492(2)		0.0238(2)	0.0241(5)	0.0240(5)	0.0232(5)	-0.0004(4)
Bi6	Bi6	0.25	0.37471(4)	0.25152(2)		0.0252(2)	0.0260(5)	0.0245(5)	0.0251(5)	-0.0015(4)
Bi7	Bi7	0.25	0.27823(4)	0.31681(2)		0.0249(2)	0.0243(5)	0.0250(5)	0.0254(5)	-0.0025(4)
Bi8	Bi8	0.75	0.44231(4)	0.32009(2)		0.0235(2)	0.0238(5)	0.0241(5)	0.0226(5)	0.0006(4)
Pb1	Pb1	0.25	0.23449(5)	0.00804(2)		0.0348(3)	0.0284(5)	0.0368(6)	0.0392(7)	-0.0045(5)
Pb2	Pb2	0.75	0.00411(5)	0.11604(2)		0.0369(3)	0.0292(6)	0.0491(7)	0.0325(6)	0.004(5)
Pb3	Pb3	0.75	0.11799(5)	0.17909(2)		0.0355(3)	0.0312(7)	0.0373(6)	0.0378(7)	-0.0043(5)
Pb4	Pb4	0.75	0.31548(5)	0.18457(2)		0.0355(3)	0.0297(6)	0.0329(6)	0.0420(7)	0.0045(5)
Pb5	Pb5	0.75	0.20538(5)	0.24985(2)		0.0355(3)	0.0334(6)	0.0435(7)	0.0296(6)	0.0038(5)
*Me*1	Me1	0.25	0.04446(4)	0.02586(2)	0.854(5)	0.0325(5)	0.0339(8)	0.0322(9)	0.0315(9)	-0.0041(6)
*Me*2	Me2	0.25	0.42113(4)	0.00591(2)		0.0305(3)	0.0229(5)	0.0344(6)	0.03437	0.0000(5)
*Me*3	Me3	0.75	0.32724(5)	0.37970(2)		0.0305(3)	0.0301(5)	0.0351(6)	0.0263(6)	0.0000(5)
*Me*4	Me4	0.75	0.20482(4)	0.43785(2)		0.0247(3)	0.0239(5)	0.0269(5)	0.0233(5)	0.0026(4)
*Me*5	Me5	0.25	0.36761(4)	0.44134(2)		0.0278(3)	0.0261(5)	0.0284(6)	0.0290(6)	0.0012(4)
*Me*6a	Pb6	0.25	-0.0023(4)	0.3191(3)	0.66(3)	0.035(2)	0.0324(7)	0.029(2)	0.043(5)	-0.00356
*Me*6b	-	0.25	0.0029(7)	0.3258(3)	0.34(3)	0.035(2)	0.0324(6)	0.029(2)	0.043(5)	-0.00356
*Me*7a	Pb7	0.25	0.1385(5)	0.3691(5)	0.83(3)	0.041(1)	0.0467(7)	0.049(4)	0.0285(7)	0.001(1)
*Me*7b	-	0.25	0.1187(2)	0.3692(3)	0.17(3)	0.041(1)	0.0467(7)	0.049(4)	0.0285(7)	0.001(1)
*Me*8a	Pb8	0.25	0.0297(5)	0.4288(1)	0.76(3)	0.037(1)	0.0324(6)	0.039(3)	0.040(2)	0.006(2)
*Me*8b	-	0.25	0.0453(8)	0.4332(3)	0.24(3)	0.037(1)	0.0324(6)	0.039(3)	0.040(2)	0.006(2)
(Cu,Fe)a	Cu,Fe	0.75	0.134(3)	0.304(2)	0.55(9)	0.032(8)	0.030(2)	0.03(2)	0.04(2)	0.01(1)
(Cu,Fe)b	-	0.75	0.144(4)	0.307(2)	0.45(9)	0.032(8)	0.030(2)	0.03(2)	0.04(2)	0.01(1)
Cu1	-	0.25	0.0828(9)	0.0112(4)	0.18(1)	0.036(8)				
Cu2	-	0.25	-0.002(1)	0.0457(5)	0.11(1)	0.03(1)				
S1		0.75	0.1345(3)	0.0220(1)		0.025(1)	0.029(3)	0.032(4)	0.016(3)	0.003(3)
S2		0.75	0.3242(3)	0.0184(1)		0.024(1)	0.025(3)	0.025(3)	0.022(3)	0.009(3)
S3		0.25	0.0654(3)	0.0756(1)		0.024(1)	0.026(3)	0.026(3)	0.021(3)	0.001(3)
S4		0.25	0.2393(3)	0.0642(1)		0.026(1)	0.023(3)	0.023(3)	0.032(4)	0.003(3)
S5		0.25	0.4160(3)	0.0658(1)		0.030(2)	0.031(4)	0.029(4)	0.029(4)	0.003(3)
S6		0.75	0.1412(3)	0.1245(1)		0.022(1)	0.023(3)	0.026(3)	0.018(3)	-0.003(3)
S7		0.75	0.3157(3)	0.1254(1)		0.028(2)	0.029(3)	0.024(3)	0.032(4)	0.000(3)
S8		0.75	0.4908(3)	0.1233(1)		0.027(2)	0.025(3)	0.027(3)	0.029(4)	0.005(3)
S9		0.25	0.0348(3)	0.1525(1)		0.022(1)	0.023(3)	0.021(3)	0.024(4)	0.002(3)
S10		0.25	0.2180(3)	0.1719(1)		0.025(1)	0.027(3)	0.026(3)	0.020(3)	-0.002(3)
S11		0.25	0.4081(3)	0.1711(1)		0.021(1)	0.024(3)	0.020(3)	0.019(3)	0.000(3)
S12		0.25	0.1330(3)	0.2215(1)		0.021(1)	0.020(3)	0.027(3)	0.0141(3)	0.001(3)
S13		0.25	0.2805(3)	0.2261(1)		0.025(1)	0.026(3)	0.025(3)	0.024(4)	0.002(3)
S14		0.75	0.4170(3)	0.2246(1)		0.021(1)	0.023(3)	0.021(3)	0.021(3)	0.005(3)
S15		0.75	0.0607(3)	0.2751(1)		0.031(2)	0.024(3)	0.039(4)	0.0290(4)	-0.001(3)
S16		0.25	0.1819(3)	0.2926(1)		0.024(1)	0.024(3)	0.020(3)	0.027(4)	-0.003(3)
S17		0.75	0.3227(3)	0.2861(1)		0.027(1)	0.025(3)	0.034(4)	0.022(4)	0.003(3)
S18		0.25	0.4882(3)	0.2917(1)		0.025(1)	0.020(3)	0.033(4)	0.023(4)	0.004(3)
S19		0.75	0.0800(3)	0.3392(1)		0.026(1)	0.028(3)	0.030(4)	0.021(3)	-0.005(3)
S20		0.75	0.2303(3)	0.3472(1)		0.031(2)	0.027(3)	0.031(4)	0.035(4)	0.010(3)
S21		0.25	0.3920(3)	0.3530(1)		0.023(1)	0.027(3)	0.024(3)	0.017(3)	0.001(3)
S22		0.75	0.1034(3)	0.4085(1)		0.025(1)	0.023(3)	0.029(4)	0.022(4)	0.001(3)
S23		0.25	0.2693(3)	0.4056(1)		0.025(1)	0.021(3)	0.030(4)	0.023(4)	0.003(3)
S24		0.75	0.4190(3)	0.4118(1)		0.030(1)	0.028(3)	0.026(4)	0.037(4)	0.008(3)
S25		0.75	0.0364(3)	0.4761(1)		0.028(2)	0.032(4)	0.027(4)	0.025(4)	0.002(3)
S26		0.25	0.1636(3)	0.4646(1)		0.030(2)	0.022(3)	0.036(4)	0.031(4)	0.013(3)
S27		0.75	0.3068(3)	0.4666(1)		0.024(1)	0.030(3)	0.023(3)	0.020(3)	0.000(3)
S28		0.25	0.4629(3)	0.4731(1)		0.031(2)	0.037(4)	0.030(4)	0.026(4)	-0.003(3)

* K1984 represents the labels of Kupčík (1984). U_{12} = 0 and U_{23} = 0 by symmetry. Occupancies of mixed *Me* sites are discussed in the text; sof: site-occupancy factor.

TABLE 4. SELECTED CATION–ANION DISTANCES (Å) IN ECLARITE

Bi1-		Bi2-		Bi3-		Bi4-		Bi5-		Bi6-	
S1	2.645(6)	S2	2.598(6)	S10	2.538(6)	S11	2.617(6)	S12	2.573(7)	S13	2.551(7)
S3	2.766(5) ×2	S5	2.785(5) ×2	S6	2.739(5) ×2	S8	2.740(5) ×2	S15	2.670(5) ×2	S14	2.673(4) ×2
S4	2.912(5) ×2	S4	2.904(5) ×2	S7	2.916(5) ×2	S7	2.926(5) ×2	S18	3.029(5) ×2	S17	3.003(5) ×2
S6	2.976(6)	S7	3.270(7)	S4	3.370(7)	S5	3.137(7)	S14	3.149(7)	S18	3.384(7)
Bi7-		Bi8-		Pb1	-	Pb2-		Pb3-		Pb4-	
S16	2.556(7)	S9	2.578(7)	S2	2.920(5) ×2	S9	2.919(4) ×2	S6	3.027(6)	S11	3.004(5) ×2
S17	2.810(5) ×2	S18	2.748(5) ×2	S4	3.069(7)	S21	3.056(7)	S10	3.061(5) ×2	S10	3.072(5) ×2
S20	2.827(5) ×2	S21	2.932(5) ×2	S1	3.129(5) ×2	S6	3.146(7)	S12	3.087(5) ×2	S13	3.135(5) ×2
S21	3.252(7)	S17	3.290(7)	S27	3.172(5) ×2	S24	3.179(5) ×2	S9	3.120(5) ×2	S14	3.177(7)
				S26	3.313(7)	S3	3.297(5) ×2	S18	3.351(7)	S7	3.232(7)
Pb5-		*Me*1-		*Me*2-		*Me*3-		*Me*4-		*Me*5-	
S13	2.942(5) ×2	S28	2.737(5) ×2	S25	2.763(5) ×2	S24	2.722(7)	S26	2.660(5) ×2	S28	2.773(7)
S12	3.028(5) ×2	S3	2.759(6)	S25	2.795(7)	S23	2.792(5) ×2	S27	2.797(7)	S27	2.805(5) ×2
S16	3.130(5) ×2	S1	2.878(5) ×2	S26	2.964(7)	S20	2.829(7)	S22	2.808(7)	S24	2.833(5) ×2
S17	3.318(7)	S28	2.886(7)	S2	3.061(5) ×2	S21	2.890(5) ×2	S23	3.050(5) ×2	S23	2.964(7)
S15	3.563(7)			S5	3.275(7)						
*Me*6a-		*Me*7a-		*Me*8a-		(Cu,Fe)a-					
S11	2.913(9) ×2	S19	2.914(7) ×2	S22	2.843(9) ×2	S19	2.28(8)				
S19	2.959(10) ×2	S22	3.054(6) ×2	S8	2.977(10)	S15	2.29(8)				
S14	3.009(15)	S20	3.137(9) ×2	S25	3.282(8) ×2	S16	2.37(4) ×2				
S8	3.152(18)	S8	3.379(13)	S5	3.288(10) ×2	S20	3.22(8)				
S15	3.446(13) ×2	S23	3.578(12)	S26	3.615(12)						
*Me*6b-		*Me*7b-		*Me*8b-		(Cu,Fe)b-		Cu1-		Cu2-	
S19	2.768(12) ×2	S19	2.739(15) ×2	S22	2.760(13) ×2	S19	2.28(14)	S28	2.325(23)	S3	2.242(28)
S8	2.796(18)	S8	2.933(34)	S25	3.098(13) ×2	S16	2.33(7) ×2	S1	2.405(12) ×2	S28	2.397(15) ×2
S11	2.953(13) ×2	S22	2.968(13) ×2	S26	3.187(19)	S15	2.57(12)	S28	3.494(18) ×2	S24	2.930(28)
S14	3.374(17)	S20	3.452(26) ×2	S8	3.322(18)	S20	2.94(12)	S3	3.541(23)	S1	3.921(24) ×2
S15	3.666(15) ×2			S5	3.561(16) ×2						

Within the error bounds of the regression with the given correlation-factor, we can postulate that the two end-member values are 1 atom Fe and 1.5 atoms Cu *pfu*, respectively. Therefore, the result of these calculations indicates that the amount of copper in surplus of the simple model structure of Kupčík (1984) is correlated with the degree of Cu-for-Fe substitution at the tetrahedral site. The compositional data obtained by Pršek *et al*. (2008) show a greater spread, but lie approximately along the trend defined by our data, in the direction of Cu contents higher than observed by us. Pršek's limit is close to the (Cu+Fe) total equal to 1.40 atoms *pfu*, whereas the present interval is defined by the boundary values of (Cu+Fe) equal to 1.10 and 1.25 atoms *pfu*. Moëlo *et al*. (1995) noticed the excess copper in the published compositions of eclarite, but in the absence of detailed structural data, they were not able to give a structural explanation for its role.

In the triangular diagram (Fig. 2), the two full circles (nos. 1 and 2) represent end-members of the coupled substitution $Cu^{+} + Bi^{3+} = Fe^{2+} + Pb^{2+}$, which was already assumed by Kupčík (1984) and Pršek *et al*. (2008). The trend suggested by our analytical results clearly deviates from the Cu-for-Fe substitution line toward higher values of the Cu:Bi ratio. Supported by the results in the Cu(*pfu*) – Fe(*pfu*) binary diagram, except for a small experimental shift, we assume that the analytical data in Figure 2 are situated on a trend anchored on the copper-free $FePb_9Bi_{12}S_{28}$ composition and pointing toward a fully developed cuprian end-member exhibiting both the Cu-for-Fe and Cu-for-Bi substitutions. Two model end-members of this type were tried, one with 0.25 Bi replaced by 0.5 Cu, and the other with 0.5 Bi replaced by 1 Cu. In both models, the tetrahedral position is fully occupied by copper. The respective model formulae are $Cu_{1.5}Pb_{7.75}Bi_{13.0}S_{28}$ and $Cu_2Pb_{7.5}Bi_{13.0}S_{28}$, *i.e*., 6.74 at.% Cu, 34.83 at.% Pb, 58.43 at.% Bi for the former and 8.89 at.% Cu, 33.34 at.% Pb, 57.78 at.% Bi for the latter end-member.

The observed trend of the structurally analyzed sample in Figures 2 and 3 coincides clearly with the former case, as does also the general trend of all our microprobe results. The data of Paar *et al*. (1983) and Pršek *et al*. (2008) are aligned in a similar way, but are too scattered to be considered in detail. In spite of a large scatter of data, further diagrams (not reproduced) show that within the accuracy of the dataset concerning rather small changes in concentrations of the large cations in the substitution process, the total amount of (Pb + Bi + Ag) *pfu* is not an obvious function of Cu

TABLE 5. CHARACTERISTICS OF COORDINATION POLYHEDRA OF CATIONS IN ECLARITE

1	2	3	4	5	6	7	8	9
Bi1	6	2.837	0.020	0.205	0.989	95.644	29.831	2.957
Bi2	6	2.889	0.020	0.323	0.968	101.032	31.521	2.849
Bi3	6	2.885	0.021	0.388	0.946	100.614	31.349	3.086
Bi4	6	2.861	0.018	0.283	0.982	98.136	30.682	2.960
Bi5	6	2.858	0.018	0.371	0.982	97.746	30.560	3.132
Bi6	6	2.893	0.022	0.413	0.945	101.471	31.578	3.125
Bi7	6	2.865	0.022	0.326	0.968	98.511	30.675	3.070
Bi8	6	2.889	0.020	0.352	0.962	100.974	31.495	2.946
Pb1	8	3.102	0.032	0.136	0.907	125.003	52.470	1.899
Pb2	8	3.122	0.030	0.205	0.954	127.485	53.606	1.823
Pb3	8	3.114	0.029	0.124	0.944	126.521	53.250	1.790
Pb4	8	3.104	0.031	0.020	0.923	125.250	52.622	1.828
Pb5	8	3.120	0.037	0.231	0.858	127.210	53.130	1.850
*Me*1	8	2.810	0.002	0.125	0.993	92.965	29.540	3.002
*Me*2	7	2.955	0.109	0.262	0.933	108.109	36.437	2.407
*Me*3	6	2.820	0.005	0.094	0.965	93.978	29.755	2.708
*Me*4	6	2.837	0.007	0.267	0.981	95.693	30.233	2.780
*Me*5	6	2.833	0.001	0.099	0.971	95.235	30.283	2.590
*Me*6a	8	3.104	0.041	0.233	0.845	125.309	52.098	2.075
*Me*6b	8	3.104	0.041	0.447	0.845	125.310	52.098	2.503
*Me*7a	8	3.151	0.055	0.203	0.822	130.990	53.669	1.838
*Me*7b	7	3.084	0.197	0.362	0.851	122.864	37.316	2.376
*Me*8a	8	3.167	0.044	0.284	0.836	133.059	55.135	1.826
*Me*8b	8	3.167	0.044	0.340	0.836	133.059	55.135	2.022
(Cu,Fe)a	4	2.335	0.054	0.094	1.000	53.342	6.185	1.133
(Cu,Fe)b	4	2.335	0.054	0.274	1.000	53.342	6.185	2.323
Cu1	4	2.806	0.349	0.756	1.000	92.544	7.385	0.755
Cu2	4	2.424	0.040	0.541	1.000	59.655	7.015	0.880

The polyhedron characteristics used were defined by Balić-Žunić & Makovicky (1996) and Makovicky & Balić-Žunić (1998). 1) site labeling, 2) coordination number, 3) radius r_s of a circumscribed sphere (in Å), least-squares-fitted to the coordination polyhedron, 4) "volume-based" distortion u = [V(ideal polyhedron) – V(real polyhedron)]/V(ideal polyhedron); the ideal polyhedron has the same number of ligands, 5) "volume-based" eccentricity $ECC_v = 1 - [(r_s - \Delta)/r_s]^3$; Δ is the distance between the center of the sphere and the central atom in the polyhedron, 6) "volume-based" sphericity $SPH_v = 1 - 3\sigma_r r_s$; σ_r is a standard deviation of the radius r_s, 7) volume of the circumscribed sphere (in Å^3), 8) volume of coordination polyhedron (in Å^3), 9) bond-valence sum.

or Fe contents. They also indicate a positive correlation between the minor increments in Ag and the total contents of Cu, and, as expected, negative correlations between the contents of Fe and Bi, and Cu and Pb, respectively, together with the opposite trends for Cu *versus* Bi and Fe *versus* Pb.

The substitution of Bi in the *Me*1 site by two flanking Cu atoms creates a deficit in positive charge, which can be compensated by increased Bi contents in the adjacent *Me*5 sites, with a mixed character. Substitutions at the three mixed sites *Me*6–8 and the (Cu,Fe) tetrahedron can be correlated and become involved in mutual compensation of valences. Significantly, there is an approximate correlation between the Cu contents of the split tetrahedral site and the sum of the site-occupancy factors for the bismuth-like positions *Me*6b and *Me*7b. Thus, both observed substitutions lead to the change in the overall Bi:Pb ratio in favor of bismuth.

Increase in the Cu content of eclarite may reflect an increased role of copper in the parent hydrothermal solutions as well as the changes in their redox potential. A structural explanation of the conspicuous correlation between the two mechanisms of substitution may be that the atom groups in question are situated on common (012) and (01$\bar{2}$) planes, which form a grid and delineate rectangular blocks of immutable portions of the structure. On every such plane, the sequence –S28–S28–*Me*5–*Me*7–*Me*6–Bi6–Bi7–*Me*7–*Me*8–S25–S25– contains the (*Me*1, Cu1,Cu2) group, a mixed site *Me*5, mixed sites *Me*7 and *Me*6 connected with the tetrahedral (Cu,Fe) site, two lone- electron-pair cations Bi6 and Bi7, and again the mixed sites *Me*7 and *Me*8. Only simultaneous substitution of Pb by Bi in all the mixed (Pb,Bi) sites mentioned will remove the structural strain that will be caused by either type of substitution acting alone. The spaces accommodating the lone pairs of electrons on Bi6 and Bi7 lie along the planes defined above and presumably adjust easily to the volume changes connected with the substitutions at the mixed sites.

Chemical formula

The combination of structural and chemical information outlined and discussed in the previous section suggests that eclarite can be modeled as a substitutional-and-interstitial solid solution of two end-members, copper-free $FePb_9Bi_{12}S_{28}$ and Cu-substituted $Cu_{1.5}Pb_{7.75}Bi_{13.0}S_{28}$. If the molar proportion of the copper-rich end-member is n and that of the iron-based end-member is $(1–n)$, the general formula is $n(Cu_{1.5}Pb_{7.75}Bi_{13.0}S_{28})\bullet(1–n)(FePb_9Bi_{12}S_{28})$ or $Cu_{1.5n}Fe_{1–n}Pb_{9–1.25n}Bi_{12+n}S_{28}$. This leads to two ways of calculating the value of n from chemical analyses: if symbols of chemical elements represent their molar amounts calculated on any basis

$$\mathrm{Cu/Fe} = q_1 = 1.5n/(1 - n)$$
$$\mathrm{Pb/Bi} = q_2 = (9 - 1.25n)/(12 + n), \quad \text{giving}$$
$$n_1 = q_1/(1.5 + q_1)$$
$$n_2 = (9 - 12q_2)/(1.25 + q_2).$$

Ideally, the two estimates, n_1, and n_2, should be the same. For the chemical formula derived from our analysis of the structurally analyzed specimen (see above), q_1 is equal to 1.711 and q_2 is equal to 0.672, resulting in n_1 equal to 0.533 and n_2 equal to 0.489, *i.e.*, a satisfactory agreement indicating about 51% of the substituted Cu-based end-member. Whether the very slight variations in the position of data clusters in "Bärenbad", "Felbertal 1" and "Felbertal 2" along the ideal substitution line stem from measurement uncertainties or from slight differences in the relative intensities of the two mechanisms of substitution active in them cannot be decided from the present data.

The reviewers suggested that we broaden the interpretation of chemical data by including the kobellite – izoklakeite pair, for which Moëlo *et al.* (1995) found a rare case of surplus of Cu over the ideal formula

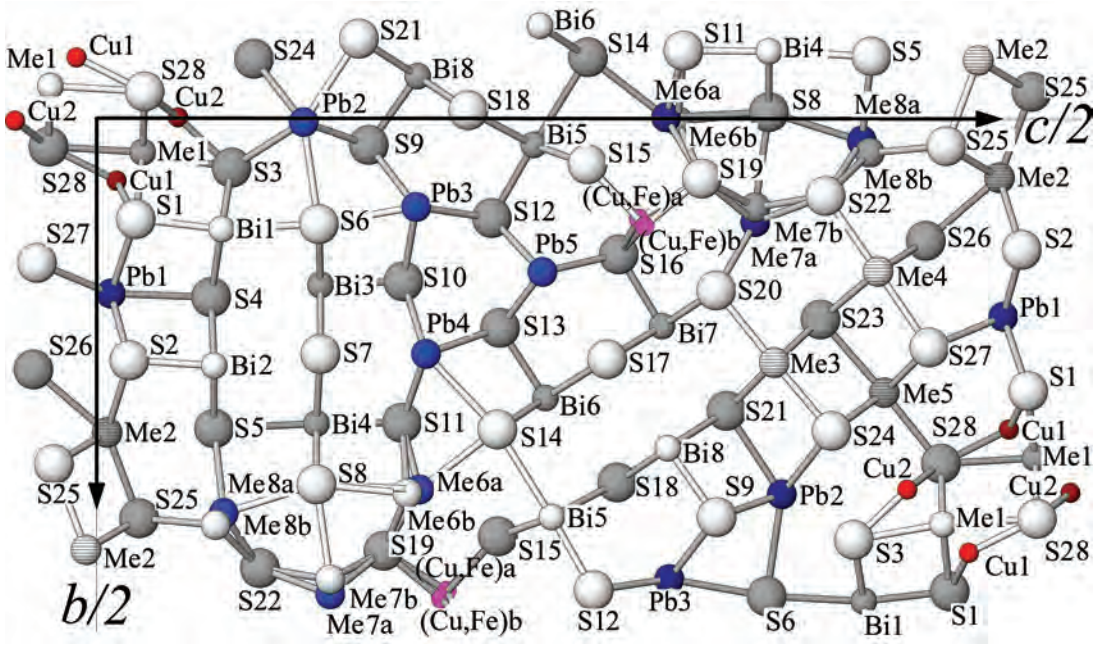

FIG. 4. Labeling of atoms in the crystal structure of eclarite. Projection on (100); the **c** axis is horizontal. Partly occupied, split and overlapping sites are discussed in the text.

derived from structure determinations. The cosalite-like *Me*1–Cu1–Cu2 configuration, however, is absent from these structures, and the interpretation of their crystal chemistry must therefore differ from that presented here for eclarite. We prefer to postpone this exercise to the time when new, highly precise determinations of the structure of kobellite and izoklakeite become available.

Comparison with previous refinements

Our data on the cation occupancies in eclarite agree in principle with those of Kupčík (1984). We also include comparisons with the conclusions from the methods based on the effects of anomalous dispersion by Wulf (1995).We started by using Kupčík's designation for atomic sites. Besides working with bond distances and polyhedron characteristics (Tables 4, 5), we used the hyperbolic dependence of opposing bond-lengths in a polyhedron of a lone-electron-pair cation, such as Pb and Bi (Fig. 6a). The references explaining this procedure in detail are Berlepsch *et al.* (2001a, 2001b). For comparison, the same scheme was constructed for the data of Kupčík (1984) (Fig. 6b); we can see a close similarity between these two datasets.

All types of data from the structure of the Felbertal eclarite confirm that *Me*1, *Me* 4, Bi3, Bi5, and Bi6 are typical Bi sites, the latter two with the most strongly expressed 3 + 2 + 1 bonding scheme. This agrees with Wulf's assignments, including that for *Me*(4), but is at variance with his mixed-site assignment of *Me*1, which is a typical Bi octahedral position in our refinement. Did its partial occupancy and surrounding Cu atoms interfere with the method Wulf was using? The next cluster of polyhedra lies slightly above the hyperbola of bismuth in Figure 6a, but in our refinement, they form a short string of in-plane values that is a secant of the hyperbola. The secant is anchored on both ends at the values 2.67 Å *versus* 3.02 Å that are derived from the array of data points in Figure 6a. If this explanation is accepted, they represent bismuth polyhedra in which occasional exchange of shorter and longer bonds in the quadratic cross-section (parallel to [100]) of the coordination octahedron takes place, *i.e.*, they are unevenly split positions. In the order of increasing deviation from the Bi hyperbola, they are the Bi4, Bi8, Bi1, Bi2, and *Me*3 sites. Similar to observations on other sulfosalts, the calculated bond-valence sum of these sites decreases in the same order, from 2.96 to 2.71. This is a region in which the largest deviations occur between our data and the refinement performed by Kupčík (1984) (Figs. 6a, b). His *R* value, however, is almost 2.5 times higher than the present one. Assignments of all these positions as bismuth agree with the conclusions of Wulf (1995).

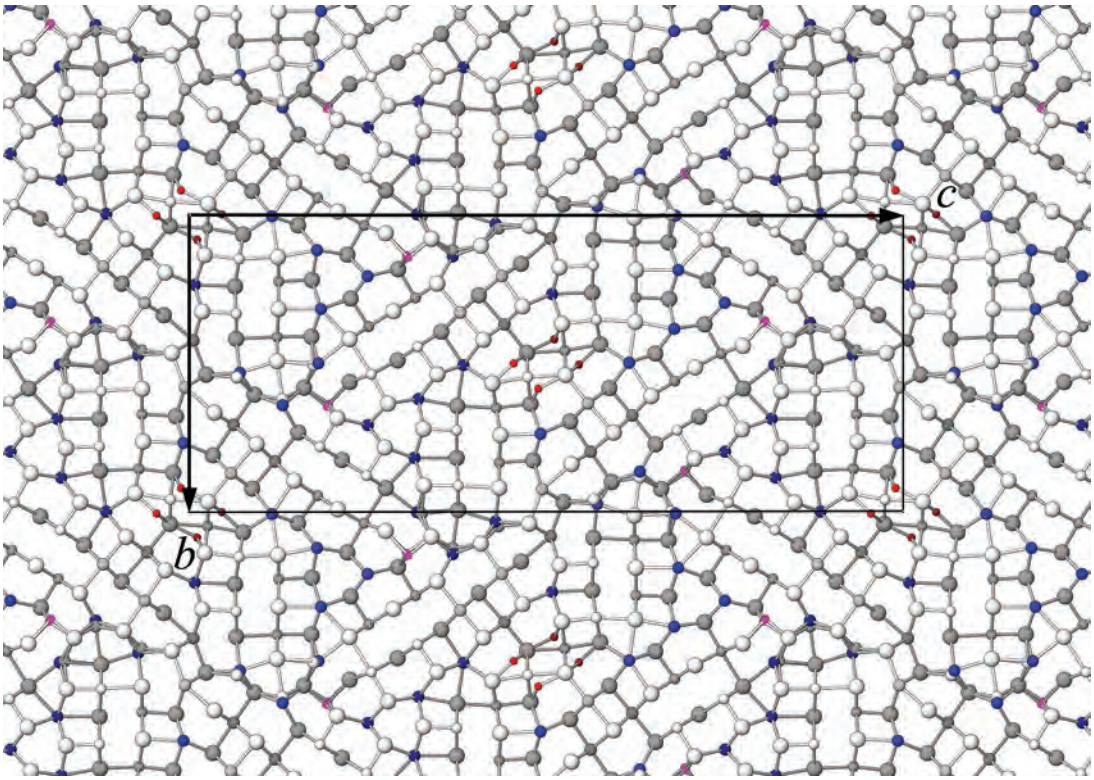

FIG. 5. The crystal structure of eclarite in projection along the 4 Å *a* period. The **c** axis is horizontal, the **b** axis is vertical. Large white spheres are S, smaller white spheres denote Bi, slightly larger (and greyish) ones are mixed (Pb,Bi) sites, Pb is dark blue, the (Cu,Fe) site is pink, and copper is rendered in red.

A clearly mixed position is *Me*2 (both the bond-valence sum of 2.41 and Wulf's conclusions concur) and, probably, one of the components of the split *Me*6 site. The latter, and the similar *Me*7 site, show a possibility of minor Bi admixture in the values of the anomalous dispersion correction term *f'* in the tabulation by Wulf (1995). All trigonal prismatic Pb sites, and the components *Me*6a–8a of the split sites, are typical lead positions; their bond-valence sums lie between 1.8 and 2.1 *vu,* whereas the *Me*6b and *Me*7b sites yield bond-valence sums of 2.5 and 2.4 *vu*.

The octahedral *Me*5 site, already discussed in connection with cosalite-like configurations, is a distorted octahedral site with in-plane configurations indicating Bi, but the out-of-plane ones are indicative of a mixed site. In the data of Wulf (1995), it is a clear Bi site; the bond-valence value in our structure determination, however, is only 2.59 *vu*. The quasi-octahedral Bi7 site has a similar symmetrical in-plane configuration but a strongly asymmetric out-of-plane one; all indications confirm a pure Bi site.

MODULAR INTERPRETATIONS

As already mentioned, Kupčík (1984) recognized and described the galena-like "regions" in the structure of eclarite and classified their interconnection as a mixture of the cosalite and kobellite principles. In his Figure 3, he attempted to clarify the situation by placing unit cells of kobellite and cosalite over the unit cells of eclarite at the right positions and in appropriate orientations.

Makovicky & Mumme (1985) noticed that in kobellite (Miehe 1971), a (010) slab of octahedra that hosts interspersed trigonal coordination prisms at ¼*b* and ¾*b* [it is a unit slice (100) of a lillianite homologue] can be left out, and the truncated structures joined, giving a motif recognizable in the structure of $Pb_4In_3Bi_7S_{18}$ (Krämer & Reis 1986). Continuing this trend, double truncation of dumbbell elements in kobellite leads to a structure reduction seen on every second such contact (010) plane in eclarite, but it gives a viable solution only where the two adjacent truncated slabs of the kobellite

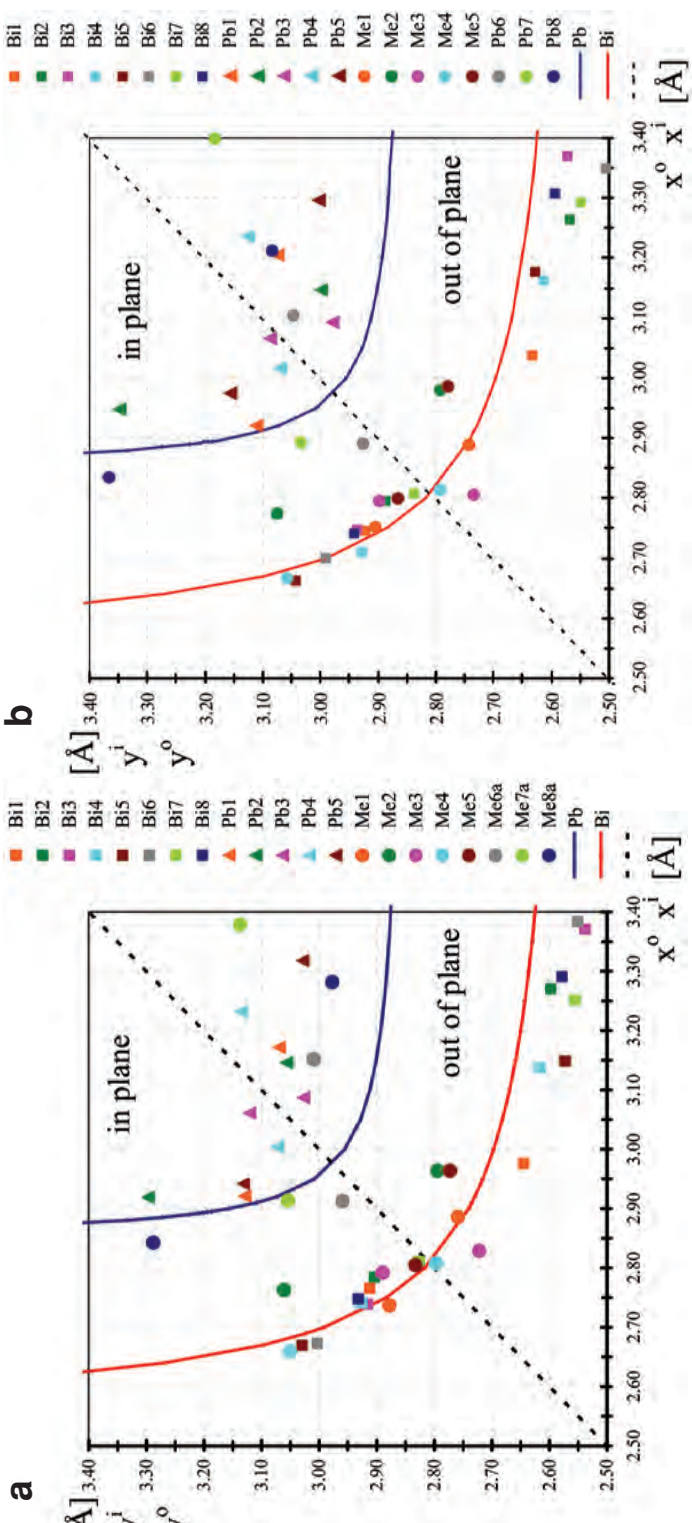

FIG. 6. Correlations of opposing bond-lengths in a bond-hyperbola plot (Berlepsch *et al.* 2001a, 2001b). (a) Our refinement data, (b) refinement by Kupčík (1984). Hyperbolae are from Berlepsch *et al.* (2001b) for Pb and from Topa *et al.* (2003) for Bi. Data points on the hyperbolae indicate Bi and Pb sites, respectively, whereas those situated between hyperbolae describe in most cases mixed-cation sites. Further details are presented in the text.

structure are shifted from the original antiphase relation to an out-of-phase relation and one slab is rotated 180° around an axis perpendicular to the composition (and truncation) plane (Fig. 7). Interconnection of these slabs then proceeds *via* two octahedra (situated between adjacent lozenge-shaped rods), two standing coordination prisms of Pb, and *via* two lying-down coordination prisms of *Me*2 that share an edge (placed between two adjacent truncated rods).

Thus, eclarite mimics a *truncation derivative of kobellite*, in which every second (010) plane of zigzag contact between rods in kobellite is reduced out into straight (010) contacts. The typical triangular columns formed by three coordination prisms of Pb, and the (Cu,Fe) tetrahedra situated in these zigzag contacts, are reduced out. The difference with kobellite is that in eclarite, the PbS archetype is used by the structure for both types of rods and not only for the larger ones.

The *cosalite-like portions* of the structure, created in the process of double truncation, display a surprisingly close similarity to the configuration observed in cosalite itself (Topa & Makovicky 2010, Srikrishnan & Nowacki 1974). This concerns the coordination and bond valence of the octahedral *Me*1 site (the calculated bond-valence value of 3.00 units), the coordination of both Cu1 and Cu2 sites, and also the coordination of the Bi1 site adjacent to the rod interconnection. They correspond to the Cu1, Cu2, *Me*2, and Bi2 sites in cosalite, respectively (Topa & Makovicky 2010). Furthermore, the coordination of the *Me*5, Pb2 and Pb3 in eclarite, in the space between the rods, corresponds fully to that observed in cosalite for *Me*1, Pb4 and Pb3. Atom Pb1 in eclarite, facing S26 and S27 across the interrod space, corresponds fully to Pb3 in cosalite, facing S6 and S8. The cosalite motif with rods having a width of N = 2 (two coordination pyramids wide), however, cannot propagate through the structure because the situation and fit seen around S27 – S1 will not be reproduced for such rod dimensions. Thus, the cosalite motif remains as an island in the structure. In the rod interior, the Bi1, Bi2, Bi3, and Bi4 sites of eclarite correspond to the Bi2, Bi1, Bi4, and *Me*3 sites of cosalite, in this order, but they do not repeat by inversion in the center of the lozenge-shaped rod as they do in cosalite, which has a rod width N = 4.

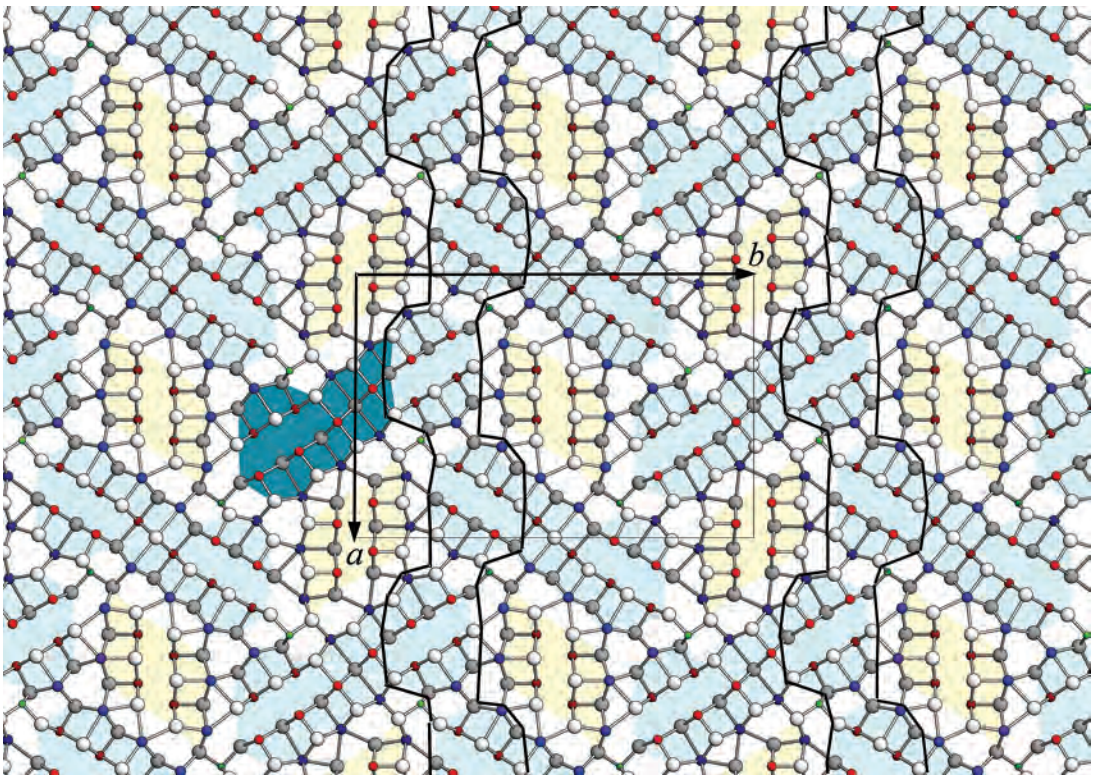

FIG. 7. The crystal structure of kobellite (Miehe 1971) with dumbbell-shaped rods indicated in light blue. One eclarite-like half-dumbbell is dark. Lozenge-shaped rods are yellow. Portions left out (*i.e.*, truncated) if the eclarite structure is modeled using kobellite as a parent structure are outlined in black. For details, see the text.

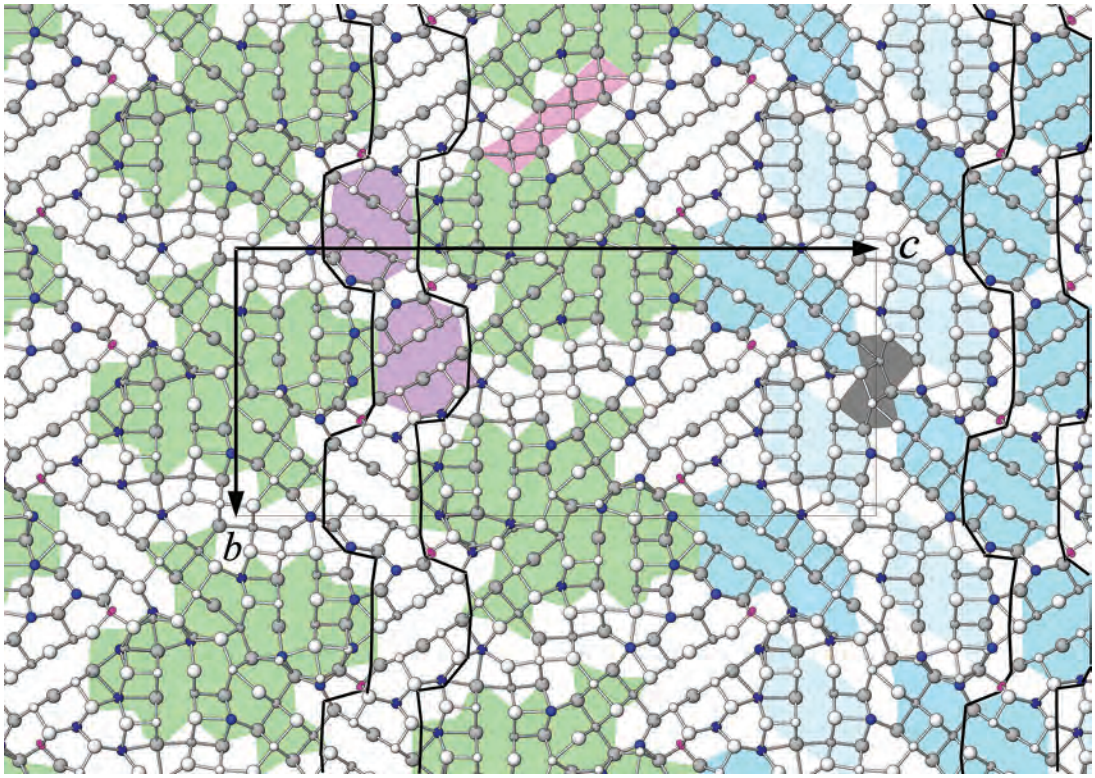

FIG. 8. Various types of structural rods ("patches" in the projection) present in the crystal structure of eclarite. Right-hand side: half-dumbbell rods: dark blue, lozenge-shaped rods: light blue, a galenobismutite-like "core element": dark grey; left-hand side: "patches" in common with galenobismutite: green, intermediate elements: pink and mauve. Portions equivalent to those eliminated on reduction from kobellite to eclarite are outlined by black lines (these are the slabs in which they are preserved!). Partially occupied copper positions in the pink-colored intermediate elements were omitted from this drawing.

We propose a completely new interpretation of the structure of eclarite, in an interesting parallel with its occurrence in the same material as galenobismutite at Felbertal. The crystal structure of eclarite contains extensive areas (rods of complicated outline) coincident with those in the crystal structure of galenobismutite. They center upon the paired columns of lying-down coordination prisms of *Me*2, evaluated as mixed (Pb,Bi) sites, which are situated at (x, ½, 0) and (x, 0, ½) of the unit cell of eclarite (Fig. 8). In galenobismutite (Fig. 9), they are centered upon (½, 0, ½) and have been named Bi3 (Pinto *et al*. 2006, Topa *et al*. 2010). The Bi–S bond lengths of these sites, forming a tightly bonded configuration, are equal to 2.79 Å and 2 × 2.76 Å, prompting Pinto *et al*. (2006) to suggest that Bi3 is a mixed Bi,Pb site. In eclarite, the bond lengths are almost identical, 2.795 Å and 2 × 2.763 Å. In galenobismutite, this core is surrounded by the Pb1–Bi2 pair on all four sides; this corresponds to twice *Me*8–Bi2 and twice Pb1–*Me*4 in eclarite (Fig. 4). The former group is extended in eclarite along the [001] direction by inclusion of Bi2, *Me*8, Bi3, Bi4, *Me*6, and Pb4. The Pb4 position already corresponds to a Bi3 site in the adjacent cell of galenobismutite along [±100]. The latter group has only *Me*3 and *Me*5 as extensions (Figs. 4, 5); it stops short of the Bi3 site in galenobismutite. Thus, there are two galenobismutite-like rods with irregular boundaries in a unit cell of eclarite (green in Fig. 8). They do not overlap and are separated by walls composed of four octahedra in the [010] direction (mauve in Fig. 8) and by truncated rods of PbS-like structure in the [0±11] directions (purple in Fig. 8). In galenobismutite itself, the "green" rod occupies nearly the entire unit-cell; rods from five adjacent cells overlap tightly (Fig. 10), leaving only "cores" of Bi3–Bi3 columns unaffected. These cores, however, are centers of other "green" rods whose outlines were not plotted in Figure 7 for the sake of clarity.

The role of the Bi3–Pb1 cluster in galenobismutite as a nucleus for more complex structures has already

been a center of attention of Makovicky (1992), who found it, *e.g.*, in $Pb_4In_3Bi_7S_{18}$ (Krämer & Reis 1986) and in sulfides of rare earths, such as $Er_9La_{10}S_{27}$ (Carré & Laruelle 1973) and $CeTmS_3$ (Rodier 1973). In these structures, they compose walls. The crystal structure of Gd_2S_3 consists entirely of such groups in different orientations (Makovicky 1992). A more recent reference to these groups is by Iordanidis & Kanatzidis (2001), as a Gd_2S_3-type building block in the crystal structures of $Pb_2La_xBi_{8-x}S_{14}$ and $La_4Bi_2S_9$. It consists of mixed (Pb,Bi,La) sites in the structure of $Pb_2La_xBi_{8-x}S_{14}$ and is situated in the intersection of walls that are two atomic planes thick. In eclarite, these groups act as nuclei of extensive, non-connected galenobismutite-like rods.

Thus, we may conclude this analysis by stating that the remarkable structure of eclarite includes principles of three important structure families, those of kobellite, cosalite and galenobismutite in a compatible combination. Copper plays a double role in the structure of eclarite, respectively corresponding to that seen in kobellite and that active in cosalite.

Acknowledgements

This research has been funded by the The Research Council for Nature and Universe (Denmark) under project no. 272–08–0227 and by the Christian Doppler Foundation (Austria). The sample studied was kindly provided by Mr. Strasser, a mineral collector from Salzburg. We express our posthumous appreciation to Prof. Vladimír Kupčík who, with the much less-well-developed methods of the day, solved this large structure. He wrote in 1984: "the direct methods led to eleven nearly isovectorial solutions"; he had to analyze them one by one in order to arrive at the right solution. We thank Dr. Y. Moëlo (Nantes) and Dr. J. Sejkora (Prague) for constructive reviews, and Prof. R.F. Martin for a thoughtful review and editorial assistance.

References

Armbruster, T. & Hummel, W. (1987): (Sb,Bi,Pb) ordering in sulfosalts: crystal-structure refinement of a Bi-rich izoklakeite. *Am. Mineral.* **72**, 821-831.

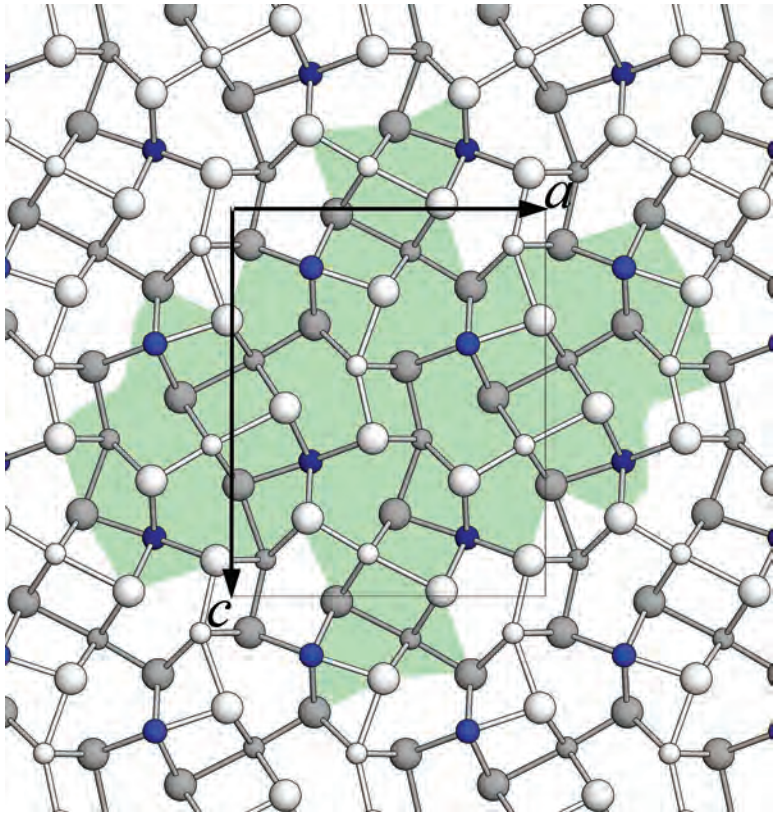

Fig. 9. A complex-structure [010] rod in the "parent" structure of galenobismutite (Topa *et al.* 2010) defined in the present paper.

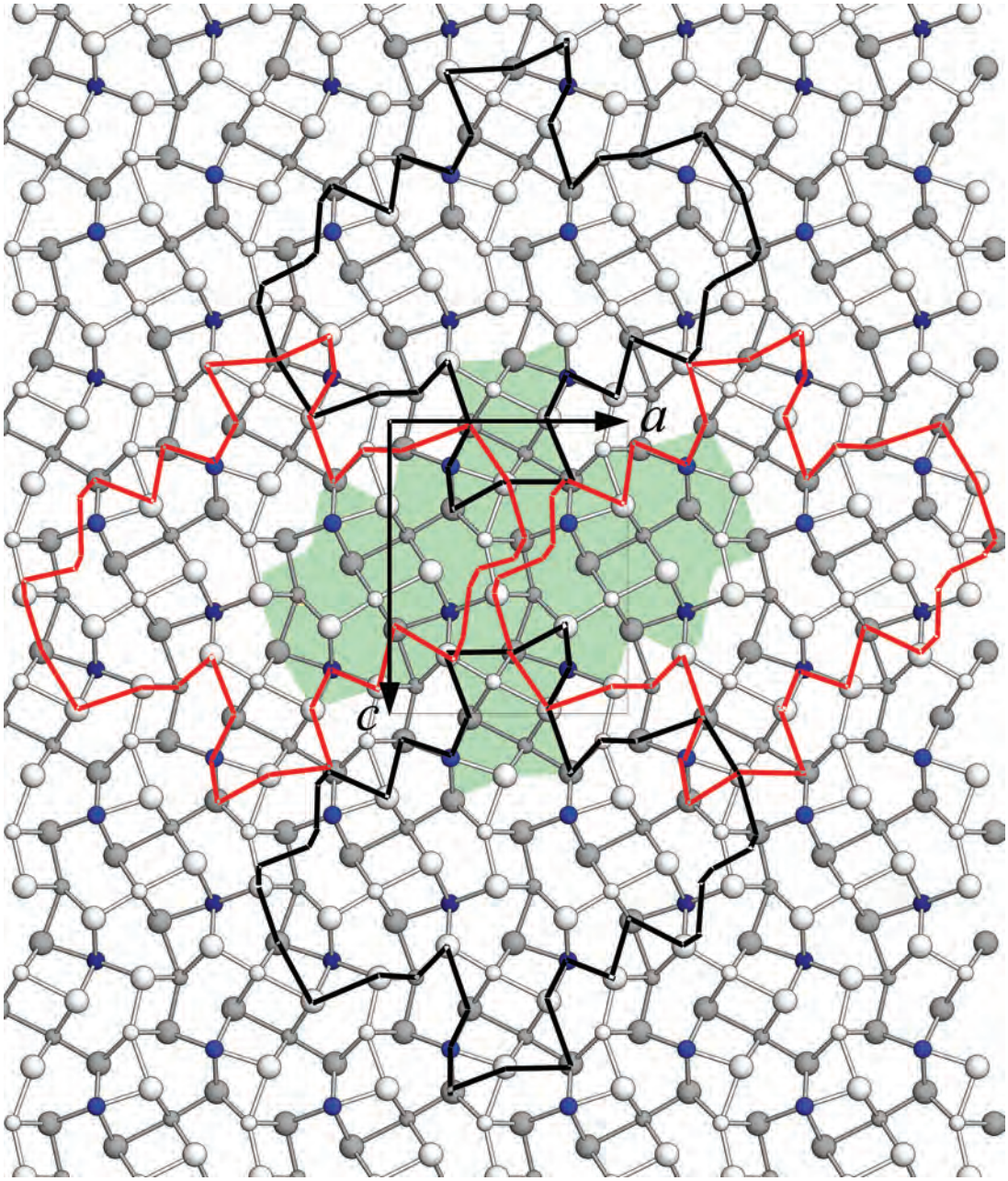

FIG. 10. The structure of galenobismutite showing the composition and overlap of several structural rods defined in Figure 9. In both figures, positions predominantly occupied by lead are shown in blue, and those predominantly occupied by Bi, in white.

BALIĆ-ŽUNIĆ, T. & MAKOVICKY, E. (1996): Determination of the centroid or "the best centre" of a coordination polyhedron. *Acta Crystallogr.* **B52**, 78-81.

BALIĆ-ŽUNIĆ, T. & VICKOVIĆ, I. (1996): IVTON – program for the calculation of geometrical aspects of crystal structures and some crystal chemical applications. *J. Appl. Crystallogr.* **29**, 305-306.

BERLEPSCH, P., MAKOVICKY, E. & BALIĆ-ŽUNIĆ, T. (2001a): Crystal chemistry of sartorite homologues and related sulfosalts. *Neues Jahrb. Mineral., Monatsh.*, 45-66.

BERLEPSCH, P., MAKOVICKY, E. & BALIĆ-ŽUNIĆ, T. (2001b): Crystal chemistry of meneghinite homologues and related sulfosalts. *Neues Jahrb. Mineral., Monatsh.*, 115-135.

BRUKER AXS (1997): SHELXTL, Version 5.1. Bruker AXS, Inc., Madison,Wisconsin 53719, USA.

BRUKER AXS (1998a): SMART, Version 5.0. Bruker AXS, Inc., Madison, Wisconsin 53719, USA.

BRUKER AXS (1998b): SAINT, Version 5.0. Bruker AXS, Inc., Madison,Wisconsin 53719, USA.

BRUKER AXS (1998c): XPREP, Version 5.0. Bruker AXS, Inc., Madison,Wisconsin 53719, USA.

CARRÉ, D. & LARUELLE, P. (1973): Structure cristalline du sulfure d'erbium et de lanthane, $Er_9La_{10}S_{27}$. *Acta Crystallogr.* **B29**, 70-73.

IORDANIDIS, L. & KANATZIDIS, M.G. (2001): Novel quaternary lanthanum bismuth sulfides $Pb_2La_xBi_{8-x}S_{14}$, $Sr_2La_xBi_{8-x}S_{14}$, and $Cs_2La_xBi_{10-x}S_{16}$ with complex structures. *Inorg. Chem.* **40**, 1878-1887.

KRÄMER, V. & REIS, I. (1986): Lead bismuth indium chalcogenides. II. Structure of $Pb_4In_3Bi_7S_{18}$. *Acta Crystallogr.* **C42**, 249-251.

KUPČÍK, V. (1984): Die Kristallstruktur des Minerals Eclarit, $(Cu,Fe)Pb_9Bi_{12}S_{28}$. *Tschermaks Mineral. Petrogr. Mitt.* **32**, 259-269.

MAKOVICKY, E. (1992): Crystal structures of complex lanthanide sulfides with built-in non-commensurability. *Aust. J. Chem.* **45**, 1451-1472.

MAKOVICKY, E. (1993): Rod-based sulphosalt structures derived from the SnS and PbS archetypes. *Eur. J. Mineral.* **5**, 545-591.

MAKOVICKY, E. & BALIĆ-ŽUNIĆ, T. (1998): New measure of distortion for coordination polyhedra. *Acta Crystallogr.* **B54**, 766-773.

MAKOVICKY, E. & MUMME, W.G. (1985): The crystal structure of izoklakeite, $Pb_{51.3}Sb_{20.4}Bi_{19.5}Ag_{1.2}Cu_{2.9}Fe_{0.7}S_{114}$. The kobellite homologous series and its derivatives. *Neues Jahrb. Mineral., Abh.* **153**, 121-145.

MIEHE, G. (1971): Crystal structure of kobellite. *Nature Phys. Sci.* **231**, 133-134.

MOËLO, Y., ROGER, G., MAUREL-PALACIN, D., MARCOUX, E. & LAROUSSI, A. (1995): Chemistry of Pb–(Cu, Fe)–(Sb,Bi)-sulfosalts from France and Portugal, and correlated substitutions in the Cu-poor part of the Pb_2S_2–Cu_2S–Sb_2S_3–Bi_2S_3 system. *Mineral. Petrol.* **53**, 229-250.

PAAR, W.H., CHEN, T.T., KUPČÍK, V. & HANKE, K. (1983): Eclarit, $(Cu,Fe)Pb_9Bi_{12}S_{28}$, ein neues Sulfosalz von Bärenbad, Hollersbachtal, Salzburg, Österreich. *Tschermaks Mineral. Petrogr. Mitt.* **32**, 103-110.

PINTO, D., BALIĆ-ŽUNIĆ, T., GARAVELLI, A., MAKOVICKY, E. & VURRO, F. (2006): Comparative crystal-structure study of Ag-free lillianite and galenobismutite from Vulcano, Aeolian Islands, Italy. *Can. Mineral.* **44**, 159-175.

PRŠEK, J., OZDÍN, D. & SEJKORA, J. (2008): Eclarite and associated Bi sulfosalts from the Brezno–Hviezda occurrence (Nízke Tatry Mts., Slovak Republic). *Neues Jahrb. Mineral., Abh.* **185**, 117-130.

RODIER, N. (1973): Structure cristalline du sulfure mixte de thulium et de cérium $TmCeS_3$. *Bull. Soc. fr. Minéral. Cristallogr.* **96**, 350-355.

SHELDRICK, G.M. (1997a): SHELXS–97. A *Computer Program for Crystal Structure Determination*. University of Göttingen, Göttingen, Germany.

SHELDRICK, G.M. (1997b): SHELXL–97. *A Computer Program for Crystal Structure Refinement*. University of Göttingen, Göttingen, Germany.

SRIKRISHNAN, T. & NOWACKI, W. (1974): A redetermination of the crystal structure of cosalite, $Pb_2Bi_2S_5$. *Z. Kristallogr.* **140**, 114-136.

TOPA, D. (2001): *Mineralogy, Crystal Structure and Crystal Chemistry of the Bismuthinite–Aikinite Series from Felbertal, Austria*. Ph.D. thesis, Institute of Mineralogy, University of Salzburg, Austria.

TOPA, D. & MAKOVICKY, E. (2010): The crystal chemistry of cosalite based on new electron-microprobe data and single-crystal determinations of the structure. *Can. Mineral.* **48**, 1081-1107.

TOPA, D., MAKOVICKY, E. & BALIĆ-ŽUNIĆ, T. (2003): Crystal structures and crystal chemistry of the members of the cuprobismutite homologous series of sulfosalts. *Can. Mineral.* **41**, 1481-1501.

TOPA, D., MAKOVICKY, E. & PUTZ, H. (2010): The crystal structure of angelaite $Cu_2AgPbBiS_4$. *Can. Mineral.* **48**, 145-153.

WULF, R. (1995): Experimental distinction of elements with similar atomic number in (Pb,Bi)-sulfosalts. *Mineral. Petrol.* **52**, 187-196.

ZAKRZEWSKI, M.A. & MAKOVICKY, E. (1986): Izoklakeite from Vena, Sweden, and the kobellite homologous series. *Can. Mineral.* **24**, 7-18.

Received November 6, 2010, revised manuscript accepted April 21, 2012.

```
data_eclarite

_audit_creation_method            SHELXL-97
_chemical_name_systematic
;
 ?
;
_chemical_name_common             ?
_chemical_melting_point           ?
_chemical_formula_moiety          ?
_chemical_formula_sum
 'Ag0.12 Bi12.76 Cu0.77 Fe0.45 Pb8.25 S28'
_chemical_formula_weight          5360.58

loop_
 _atom_type_symbol
 _atom_type_description
 _atom_type_scat_dispersion_real
 _atom_type_scat_dispersion_imag
 _atom_type_scat_source
 'S'  'S'   0.1246   0.1234
 'International Tables Vol C Tables 4.2.6.8 and 6.1.1.4'
 'Fe'  'Fe'   0.3463   0.8444
 'International Tables Vol C Tables 4.2.6.8 and 6.1.1.4'
 'Cu'  'Cu'   0.3201   1.2651
 'International Tables Vol C Tables 4.2.6.8 and 6.1.1.4'
 'Ag'  'Ag'  -0.8971   1.1015
 'International Tables Vol C Tables 4.2.6.8 and 6.1.1.4'
 'Pb'  'Pb'  -3.3944  10.1111
 'International Tables Vol C Tables 4.2.6.8 and 6.1.1.4'
 'Bi'  'Bi'  -4.1077  10.2566
 'International Tables Vol C Tables 4.2.6.8 and 6.1.1.4'

_symmetry_cell_setting           'Orthorhombic'
_symmetry_space_group_name_H-M   'Pmcn '

loop_
 _symmetry_equiv_pos_as_xyz
 'x, y, z'
 '-x, y+1/2, -z+1/2'
 'x+1/2, -y, -z'
 '-x+1/2, -y+1/2, z+1/2'
 '-x, -y, -z'
 'x, -y-1/2, z-1/2'
 '-x-1/2, y, z'
 'x-1/2, y-1/2, -z-1/2'

_cell_length_a                   4.03070(10)
_cell_length_b                   22.7011(6)
_cell_length_c                   54.6145(13)
_cell_angle_alpha                90.00
_cell_angle_beta                 90.00
_cell_angle_gamma                90.00
_cell_volume                     4997.3(2)
```

```
_cell_formula_units_Z            4
_cell_measurement_temperature    297(2)
_cell_measurement_reflns_used    ?
_cell_measurement_theta_min      ?
_cell_measurement_theta_max      ?

_exptl_crystal_description       ?
_exptl_crystal_colour            ?
_exptl_crystal_size_max          ?
_exptl_crystal_size_mid          ?
_exptl_crystal_size_min          ?
_exptl_crystal_density_meas      ?
_exptl_crystal_density_diffrn    7.125
_exptl_crystal_density_method    'not measured'
_exptl_crystal_F_000             8893
_exptl_absorpt_coefficient_mu    74.087
_exptl_absorpt_correction_type   ?
_exptl_absorpt_correction_T_min  ?
_exptl_absorpt_correction_T_max  ?
_exptl_absorpt_process_details   ?

_exptl_special_details
;
 ?
;

_diffrn_ambient_temperature      297(2)
_diffrn_radiation_wavelength     0.71073
_diffrn_radiation_type           MoK\a
_diffrn_radiation_source         'fine-focus sealed tube'
_diffrn_radiation_monochromator  graphite
_diffrn_measurement_device_type  ?
_diffrn_measurement_method       ?
_diffrn_detector_area_resol_mean ?
_diffrn_standards_number         ?
_diffrn_standards_interval_count ?
_diffrn_standards_interval_time  ?
_diffrn_standards_decay_%        ?
_diffrn_reflns_number            34772
_diffrn_reflns_av_R_equivalents  0.1089
_diffrn_reflns_av_sigmaI/netI    0.0570
_diffrn_reflns_limit_h_min       -4
_diffrn_reflns_limit_h_max       4
_diffrn_reflns_limit_k_min       -26
_diffrn_reflns_limit_k_max       26
_diffrn_reflns_limit_l_min       -64
_diffrn_reflns_limit_l_max       64
_diffrn_reflns_theta_min         0.97
_diffrn_reflns_theta_max         25.23
_reflns_number_total             4976
_reflns_number_gt                4141
_reflns_threshold_expression     >2sigma(I)

_computing_data_collection       ?
_computing_cell_refinement       ?
```

```
_computing_data_reduction         ?
_computing_structure_solution     'SHELXS-97 (Sheldrick, 1990)'
_computing_structure_refinement   'SHELXL-97 (Sheldrick, 1997)'
_computing_molecular_graphics     ?
_computing_publication_material   ?

_refine_special_details
;
 Refinement of F^2^ against ALL reflections.  The weighted R-factor wR and
 goodness of fit S are based on F^2^, conventional R-factors R are based
 on F, with F set to zero for negative F^2^. The threshold expression of
 F^2^ > 2sigma(F^2^) is used only for calculating R-factors(gt) etc. and is
 not relevant to the choice of reflections for refinement.  R-factors based
 on F^2^ are statistically about twice as large as those based on F, and R-
 factors based on ALL data will be even larger.
;

_refine_ls_structure_factor_coef  Fsqd
_refine_ls_matrix_type            full
_refine_ls_weighting_scheme       calc
_refine_ls_weighting_details
 'calc w=1/[\s^2^(Fo^2^)+(0.0480P)^2^+0.0000P] where P=(Fo^2^+2Fc^2^)/3'
_atom_sites_solution_primary      direct
_atom_sites_solution_secondary    difmap
_atom_sites_solution_hydrogens    geom
_refine_ls_hydrogen_treatment     mixed
_refine_ls_extinction_method      SHELXL
_refine_ls_extinction_coef        0.000008(3)
_refine_ls_extinction_expression
 'Fc^*^=kFc[1+0.001xFc^2^\l^3^/sin(2\q)]^-1/4^'
_refine_ls_number_reflns          4976
_refine_ls_number_parameters      324
_refine_ls_number_restraints      0
_refine_ls_R_factor_all           0.0584
_refine_ls_R_factor_gt            0.0454
_refine_ls_wR_factor_ref          0.1010
_refine_ls_wR_factor_gt           0.0953
_refine_ls_goodness_of_fit_ref    1.032
_refine_ls_restrained_S_all       1.032
_refine_ls_shift/su_max           0.001
_refine_ls_shift/su_mean          0.000

loop_
 _atom_site_label
 _atom_site_type_symbol
 _atom_site_fract_x
 _atom_site_fract_y
 _atom_site_fract_z
 _atom_site_U_iso_or_equiv
 _atom_site_adp_type
 _atom_site_occupancy
 _atom_site_symmetry_multiplicity
 _atom_site_calc_flag
 _atom_site_refinement_flags
 _atom_site_disorder_assembly
```

```
 _atom_site_disorder_group
Bi1 Bi 0.7500 0.14778(4) 0.070090(18) 0.0244(2) Uani 1 2 d S . .
Bi2 Bi 0.7500 0.33131(4) 0.065868(18) 0.0245(2) Uani 1 2 d S . .
Bi3 Bi 0.2500 0.22287(4) 0.125515(17) 0.0247(2) Uani 1 2 d S . .
Bi4 Bi 0.2500 0.40900(4) 0.123206(18) 0.0251(2) Uani 1 2 d S . .
Bi5 Bi 0.2500 0.03474(4) 0.244920(18) 0.0238(2) Uani 1 2 d S . .
Bi6 Bi 0.2500 0.37471(4) 0.251522(18) 0.0252(2) Uani 1 2 d S . .
Bi7 Bi 0.2500 0.27823(4) 0.316806(18) 0.0249(2) Uani 1 2 d S . .
Bi8 Bi 0.7500 0.44231(4) 0.320094(17) 0.0235(2) Uani 1 2 d S . .
ME2 Bi 0.2500 0.42113(4) 0.00591(2) 0.0305(3) Uani 1 2 d S . .
ME3 Bi 0.7500 0.32724(5) 0.379705(19) 0.0305(3) Uani 1 2 d S . .
ME4 Bi 0.7500 0.20482(4) 0.437853(18) 0.0247(2) Uani 1 2 d S . .
ME5 Bi 0.2500 0.36761(4) 0.441339(19) 0.0278(2) Uani 1 2 d S . .
Pb1 Pb 0.2500 0.23449(5) 0.00804(2) 0.0348(3) Uani 1 2 d S . .
Pb2 Pb 0.7500 0.00411(5) 0.11604(2) 0.0369(3) Uani 1 2 d S . .
Pb3 Pb 0.7500 0.11799(5) 0.17909(2) 0.0354(3) Uani 1 2 d S . .
Pb4 Pb 0.7500 0.31548(5) 0.18457(2) 0.0355(3) Uani 1 2 d S . .
Pb5 Pb 0.7500 0.20538(5) 0.24985(2) 0.0355(3) Uani 1 2 d S . .
Pb6A Pb 0.2500 -0.0023(4) 0.3191(3) 0.0347(15) Uani 0.66(3) 2 d SP . .
PB6B Bi 0.2500 0.0029(7) 0.3258(3) 0.0347(15) Uani 0.34(3) 2 d SP . .
Pb7A Pb 0.2500 0.1385(5) 0.36909(5) 0.0413(12) Uani 0.83(3) 2 d SP . .
PB7B Bi 0.2500 0.1187(15) 0.3691(3) 0.0413(12) Uani 0.17(3) 2 d SP . .
Pb8A Pb 0.2500 0.0297(5) 0.42879(14) 0.0371(12) Uani 0.76(3) 2 d SP . .
PB8B Bi 0.2500 0.0453(8) 0.4332(3) 0.0371(12) Uani 0.24(3) 2 d SP . .
Cu Cu 0.7500 0.134(3) 0.3039(16) 0.032(8) Uani 0.55(9) 2 d SP . .
Fe Fe 0.7500 0.144(4) 0.307(2) 0.032(8) Uani 0.45(9) 2 d SP . .
Bi9 Bi 0.2500 0.04446(5) 0.02586(2) 0.0325(5) Uani 0.854(5) 2 d SP . .
Cu1 Cu 0.2500 0.0828(9) 0.0112(4) 0.036(8) Uiso 0.179(14) 2 d SP . .
Cu2 Cu 0.2500 -0.0022(12) 0.0457(5) 0.030(11) Uiso 0.113(12) 2 d SP . .
S1 S 0.7500 0.1345(3) 0.02197(11) 0.0254(14) Uani 1 2 d S . .
S2 S 0.7500 0.3242(3) 0.01839(11) 0.0238(14) Uani 1 2 d S . .
S3 S 0.2500 0.0654(3) 0.07563(11) 0.0241(14) Uani 1 2 d S . .
S4 S 0.2500 0.2393(3) 0.06419(12) 0.0256(14) Uani 1 2 d S . .
S5 S 0.2500 0.4160(3) 0.06584(12) 0.0297(15) Uani 1 2 d S . .
S6 S 0.7500 0.1412(3) 0.12451(11) 0.0222(13) Uani 1 2 d S . .
S7 S 0.7500 0.3157(3) 0.12540(12) 0.0284(15) Uani 1 2 d S . .
S8 S 0.7500 0.4908(3) 0.12326(12) 0.0271(15) Uani 1 2 d S . .
S9 S 0.2500 0.0348(3) 0.15253(11) 0.0227(14) Uani 1 2 d S . .
S10 S 0.2500 0.2180(3) 0.17193(11) 0.0244(14) Uani 1 2 d S . .
S11 S 0.2500 0.4081(3) 0.17113(11) 0.0213(13) Uani 1 2 d S . .
S12 S 0.2500 0.1330(3) 0.22145(11) 0.0205(13) Uani 1 2 d S . .
S13 S 0.2500 0.2805(3) 0.22606(12) 0.0250(14) Uani 1 2 d S . .
S14 S 0.7500 0.4170(3) 0.22461(11) 0.0214(13) Uani 1 2 d S . .
S15 S 0.7500 0.0607(3) 0.27513(13) 0.0308(15) Uani 1 2 d S . .
S16 S 0.2500 0.1819(3) 0.29259(12) 0.0235(14) Uani 1 2 d S . .
S17 S 0.7500 0.3227(3) 0.28608(12) 0.0267(15) Uani 1 2 d S . .
S18 S 0.2500 0.4882(3) 0.29170(12) 0.0252(14) Uani 1 2 d S . .
S19 S 0.7500 0.0800(3) 0.33918(12) 0.0262(14) Uani 1 2 d S . .
S20 S 0.7500 0.2303(3) 0.34716(13) 0.0307(16) Uani 1 2 d S . .
S21 S 0.2500 0.3920(3) 0.35300(11) 0.0228(13) Uani 1 2 d S . .
S22 S 0.7500 0.1033(3) 0.40848(11) 0.0247(14) Uani 1 2 d S . .
S23 S 0.2500 0.2693(3) 0.40563(11) 0.0246(14) Uani 1 2 d S . .
S24 S 0.7500 0.4190(3) 0.41180(13) 0.0303(15) Uani 1 2 d S . .
S25 S 0.7500 0.0364(3) 0.47613(12) 0.0277(15) Uani 1 2 d S . .
S26 S 0.2500 0.1636(3) 0.46463(13) 0.0295(15) Uani 1 2 d S . .
```

```
S27 S 0.7500 0.3068(3) 0.46660(11) 0.0242(14) Uani 1 2 d S . .
S28 S 0.2500 0.4629(3) 0.47310(12) 0.0308(15) Uani 1 2 d S . .

loop_
 _atom_site_aniso_label
 _atom_site_aniso_U_11
 _atom_site_aniso_U_22
 _atom_site_aniso_U_33
 _atom_site_aniso_U_23
 _atom_site_aniso_U_13
 _atom_site_aniso_U_12
Bi1 0.0256(5) 0.0255(5) 0.0219(5) -0.0008(4) 0.000 0.000
Bi2 0.0258(5) 0.0259(5) 0.0218(5) 0.0006(4) 0.000 0.000
Bi3 0.0248(5) 0.0285(5) 0.0209(5) -0.0011(4) 0.000 0.000
Bi4 0.0241(5) 0.0290(5) 0.0221(5) -0.0010(4) 0.000 0.000
Bi5 0.0241(5) 0.0240(5) 0.0232(5) -0.0004(4) 0.000 0.000
Bi6 0.0260(5) 0.0245(5) 0.0251(5) -0.0015(4) 0.000 0.000
Bi7 0.0243(5) 0.0250(5) 0.0253(5) -0.0025(4) 0.000 0.000
Bi8 0.0238(5) 0.0241(5) 0.0226(5) 0.0006(4) 0.000 0.000
ME2 0.0228(5) 0.0344(6) 0.0344(6) 0.0001(5) 0.000 0.000
ME3 0.0301(5) 0.0351(6) 0.0263(6) 0.0001(5) 0.000 0.000
ME4 0.0239(5) 0.0269(5) 0.0233(5) 0.0026(4) 0.000 0.000
ME5 0.0261(5) 0.0284(6) 0.0290(6) 0.0012(4) 0.000 0.000
Pb1 0.0284(5) 0.0368(6) 0.0392(7) -0.0046(5) 0.000 0.000
Pb2 0.0292(6) 0.0491(7) 0.0325(6) 0.0040(5) 0.000 0.000
Pb3 0.0312(6) 0.0373(6) 0.0378(7) -0.0043(5) 0.000 0.000
Pb4 0.0296(6) 0.0329(6) 0.0440(7) 0.0045(5) 0.000 0.000
Pb5 0.0334(6) 0.0435(7) 0.0296(6) 0.0038(5) 0.000 0.000
Pb6A 0.0324(6) 0.0293(16) 0.042(5) -0.004(2) 0.000 0.000
PB6B 0.0324(6) 0.0293(16) 0.042(5) -0.004(2) 0.000 0.000
Pb7A 0.0467(7) 0.049(4) 0.0285(7) 0.0008(13) 0.000 0.000
PB7B 0.0467(7) 0.049(4) 0.0285(7) 0.0008(13) 0.000 0.000
Pb8A 0.0324(6) 0.039(3) 0.0402(19) 0.0055(19) 0.000 0.000
PB8B 0.0324(6) 0.039(3) 0.0402(19) 0.0055(19) 0.000 0.000
Cu 0.030(2) 0.03(2) 0.038(19) 0.007(12) 0.000 0.000
Fe 0.030(2) 0.03(2) 0.038(19) 0.007(12) 0.000 0.000
Bi9 0.0339(8) 0.0322(8) 0.0315(8) -0.0041(6) 0.000 0.000
S1 0.029(3) 0.031(4) 0.016(3) 0.003(3) 0.000 0.000
S2 0.025(3) 0.024(3) 0.022(3) 0.009(3) 0.000 0.000
S3 0.026(3) 0.025(3) 0.021(3) 0.001(3) 0.000 0.000
S4 0.023(3) 0.022(3) 0.032(4) 0.002(3) 0.000 0.000
S5 0.031(4) 0.029(4) 0.029(4) 0.003(3) 0.000 0.000
S6 0.023(3) 0.026(3) 0.018(3) 0.000(3) 0.000 0.000
S7 0.029(3) 0.024(3) 0.032(4) 0.000(3) 0.000 0.000
S8 0.025(3) 0.027(3) 0.029(4) 0.005(3) 0.000 0.000
S9 0.023(3) 0.021(3) 0.024(4) 0.002(3) 0.000 0.000
S10 0.027(3) 0.026(3) 0.020(3) -0.002(3) 0.000 0.000
S11 0.024(3) 0.021(3) 0.019(3) 0.000(3) 0.000 0.000
S12 0.020(3) 0.027(3) 0.014(3) 0.001(3) 0.000 0.000
S13 0.026(3) 0.025(3) 0.024(4) 0.002(3) 0.000 0.000
S14 0.023(3) 0.021(3) 0.020(3) 0.005(3) 0.000 0.000
S15 0.024(3) 0.039(4) 0.029(4) -0.001(3) 0.000 0.000
S16 0.024(3) 0.020(3) 0.027(4) -0.003(3) 0.000 0.000
S17 0.025(3) 0.034(4) 0.022(4) 0.003(3) 0.000 0.000
S18 0.020(3) 0.033(4) 0.023(4) 0.004(3) 0.000 0.000
```

```
S19 0.028(3) 0.030(4) 0.021(3) -0.005(3) 0.000 0.000
S20 0.026(3) 0.031(4) 0.035(4) 0.009(3) 0.000 0.000
S21 0.027(3) 0.024(3) 0.017(3) 0.000(3) 0.000 0.000
S22 0.023(3) 0.029(4) 0.022(3) 0.001(3) 0.000 0.000
S23 0.021(3) 0.030(4) 0.023(3) 0.003(3) 0.000 0.000
S24 0.028(3) 0.026(4) 0.037(4) 0.007(3) 0.000 0.000
S25 0.032(4) 0.027(4) 0.024(4) 0.002(3) 0.000 0.000
S26 0.022(3) 0.036(4) 0.031(4) 0.013(3) 0.000 0.000
S27 0.029(3) 0.023(3) 0.020(3) 0.000(3) 0.000 0.000
S28 0.037(4) 0.030(4) 0.025(4) -0.003(3) 0.000 0.000

_geom_special_details
;
 All esds (except the esd in the dihedral angle between two l.s. planes)
 are estimated using the full covariance matrix.  The cell esds are taken
 into account individually in the estimation of esds in distances, angles
 and torsion angles; correlations between esds in cell parameters are only
 used when they are defined by crystal symmetry.  An approximate (isotropic)
 treatment of cell esds is used for estimating esds involving l.s. planes.
;

loop_
 _geom_bond_atom_site_label_1
 _geom_bond_atom_site_label_2
 _geom_bond_distance
 _geom_bond_site_symmetry_2
 _geom_bond_publ_flag
Bi1 S1 2.645(6) . ?
Bi1 S3 2.766(4) . ?
Bi1 S3 2.766(4) 1_655 ?
Bi1 S4 2.912(4) 1_655 ?
Bi1 S4 2.912(4) . ?
Bi1 S6 2.976(6) . ?
Bi2 S2 2.598(6) . ?
Bi2 S5 2.785(5) 1_655 ?
Bi2 S5 2.785(5) . ?
Bi2 S4 2.904(4) . ?
Bi2 S4 2.904(4) 1_655 ?
Bi3 S10 2.537(6) . ?
Bi3 S6 2.740(4) 1_455 ?
Bi3 S6 2.740(4) . ?
Bi3 S7 2.916(5) . ?
Bi3 S7 2.916(5) 1_455 ?
Bi4 S11 2.617(6) . ?
Bi4 S8 2.740(4) . ?
Bi4 S8 2.740(4) 1_455 ?
Bi4 S7 2.926(5) 1_455 ?
Bi4 S7 2.926(5) . ?
Bi4 S5 3.137(7) . ?
Bi5 S12 2.573(6) . ?
Bi5 S15 2.670(5) . ?
Bi5 S15 2.670(5) 1_455 ?
Bi5 S18 3.029(5) 2_545 ?
Bi5 S18 3.029(5) 2_645 ?
Bi6 S13 2.551(6) . ?
```